

2

Report No. NADC-88141-60 (Volume I)



AD-A208 345

IC

CTE

MAY 26 1989

D

D

**RESIDUAL STRESS CHANGES
IN FATIGUE
VOLUME I — RESIDUAL STRESS
MEASUREMENTS BY X-RAY
DIFFRACTION IN NOTCHED
TEST SPECIMENS**

N.E. Dowling and D.O. Dunn
Engineering Science and Mechanics Department
VIRGINIA POLYTECHNIC INSTITUTE AND STATE UNIVERSITY
Blacksburg, VA 24061

Contract N62269-85-C-0256

1 MARCH 1989
INTERIM REPORT FOR PERIOD OCT. 1985 - DEC. 1987
AIRTASK NO. R02303001
Program Element No. 61153N
Work Unit No. 1EJ7AB2

Approved for Public Release;
Distribution is Unlimited

Prepared for
Air Vehicles and Crew Systems Technology Department (Code 6043)
NAVAL AIR DEVELOPMENT CENTER
Warminster, PA 18974-5000

083

NOTICES

REPORT NUMBERING SYSTEM - The numbering of technical project reports issued by the Naval Air Development Center is arranged for specific identification purposes. Each number consists of the Center acronym, the calendar year in which the number was assigned, the sequence number of the report within the specific calendar year, and the official 2-digit correspondence code of the Command Officer or the Functional Department responsible for the report. For example: Report No. NADC 88020-80 indicates the twentieth Center report for the year 1988 and prepared by the Air Vehicle and Crew Systems Technology Department. The numerical codes are as follows:

CODE	OFFICE OR DEPARTMENT
00	Commander, Naval Air Development Center
01	Technical Director, Naval Air Development Center
05	Computer Department
10	AntiSubmarine Warfare Systems Department
20	Tactical Air Systems Department
30	Warfare Systems Analysis Department
40	Communication Navigation Technology Department
50	Mission Avionics Technology Department
60	Air Vehicle & Crew Systems Technology Department
70	Systems & Software Technology Department
80	Engineering Support Group
90	Test & Evaluation Group

PRODUCT ENDORSEMENT - The discussion or instructions concerning commercial products herein do not constitute an endorsement by the Government nor do they convey or imply the license or right to use such products.

UNCLASSIFIED

SECURITY CLASSIFICATION OF THIS PAGE

REPORT DOCUMENTATION PAGE				Form Approved OMB No 0704-0188	
1a REPORT SECURITY CLASSIFICATION UNCLASSIFIED		1b RESTRICTIVE MARKINGS			
2a SECURITY CLASSIFICATION AUTHORITY		3 DISTRIBUTION / AVAILABILITY OF REPORT Approved for Public Release; Distribution Unlimited			
2b DECLASSIFICATION / DOWNGRADING SCHEDULE					
4. PERFORMING ORGANIZATION REPORT NUMBER(S)		5 MONITORING ORGANIZATION REPORT NUMBER(S) NADC-88141-60 (Vol. I)			
6a NAME OF PERFORMING ORGANIZATION Virginia Polytechnic Institute and State University		6b OFFICE SYMBOL <i>(if applicable)</i>		7a NAME OF MONITORING ORGANIZATION Air Vehicle & Crew Systems Technology Department (Code 6043) NAVAL AIR DEVELOPMENT CENTER	
6c. ADDRESS (City, State, and ZIP Code) Blacksburg, VA 24061		7b ADDRESS (City, State, and ZIP Code) Warminster, PA 18974-5000			
8a NAME OF FUNDING / SPONSORING ORGANIZATION NAVAL AIR SYSTEMS COMMAND		8b OFFICE SYMBOL <i>(if applicable)</i> AIR-931B		9 PROCUREMENT INSTRUMENT IDENTIFICATION NUMBER N62269-85-C-0256	
8c. ADDRESS (City, State, and ZIP Code) Department of the NAVY Washington, DC 20361		10 SOURCE OF FUNDING NUMBERS			
		PROGRAM ELEMENT NO 61153N	PROJECT NO	TASK NO R02303001	WORK UNIT ACCESSION NO 106352
11 TITLE (Include Security Classification) (v) Residual Stress Changes in Fatigue; Vol. II, A Simulation Model for Stress Measurements in Notched Test Specimens by X-Ray Diffraction					
12 PERSONAL AUTHOR(S) Dowling, N.E. and Dunn, D.O.					
13a TYPE OF REPORT Interim		13b TIME COVERED FROM Oct. 85 TO Sept. 87		14 DATE OF REPORT (Year, Month, Day) 1989 March 1	
15 PAGE COUNT 73					
16 SUPPLEMENTARY NOTATION This report consists of two volumes					
17 COSATI CODES			18 SUBJECT TERMS (Continue on reverse if necessary and identify by block number)		
FIELD	GROUP	SUB-GROUP			
01	03		Airframes; Fatigue (Mechanics); Fatigue Life; Predictions; Failure (Mechanics); Spectra; Computerized Simulation; Residual Stress; X-Ray Diffraction; (KT)		
20	11				
19 ABSTRACT (Continue on reverse if necessary and identify by block number)					
<p>An experimental setup is described for performing residual stress measurements on notched test specimens under load using a TEC series 1600 x-ray diffraction system. Excellent results are being obtained for Ti-6Al-4V material, but measurements on 7475-1651 Al are complicated by a texturing problem. Also, some unusual effects are observed during plastic deformation which are not yet understood. The performance of the x-ray diffraction system is found to be quite good in general, but some minor problems are noted.</p> <p><i>Keywords: stress mechanics; aluminum alloys; Titanium alloys;</i></p>					
20 DISTRIBUTION / AVAILABILITY OF ABSTRACT <input checked="" type="checkbox"/> UNCLASSIFIED/UNLIMITED <input type="checkbox"/> SAME AS RPT <input type="checkbox"/> DTIC USERS			21 ABSTRACT SECURITY CLASSIFICATION UNCLASSIFIED		
22a NAME OF RESPONSIBLE INDIVIDUAL R.E. Vining			22b TELEPHONE (Include Area Code) 215-441-2730		22c OFFICE SYMBOL 6043

DD Form 1473, JUN 86

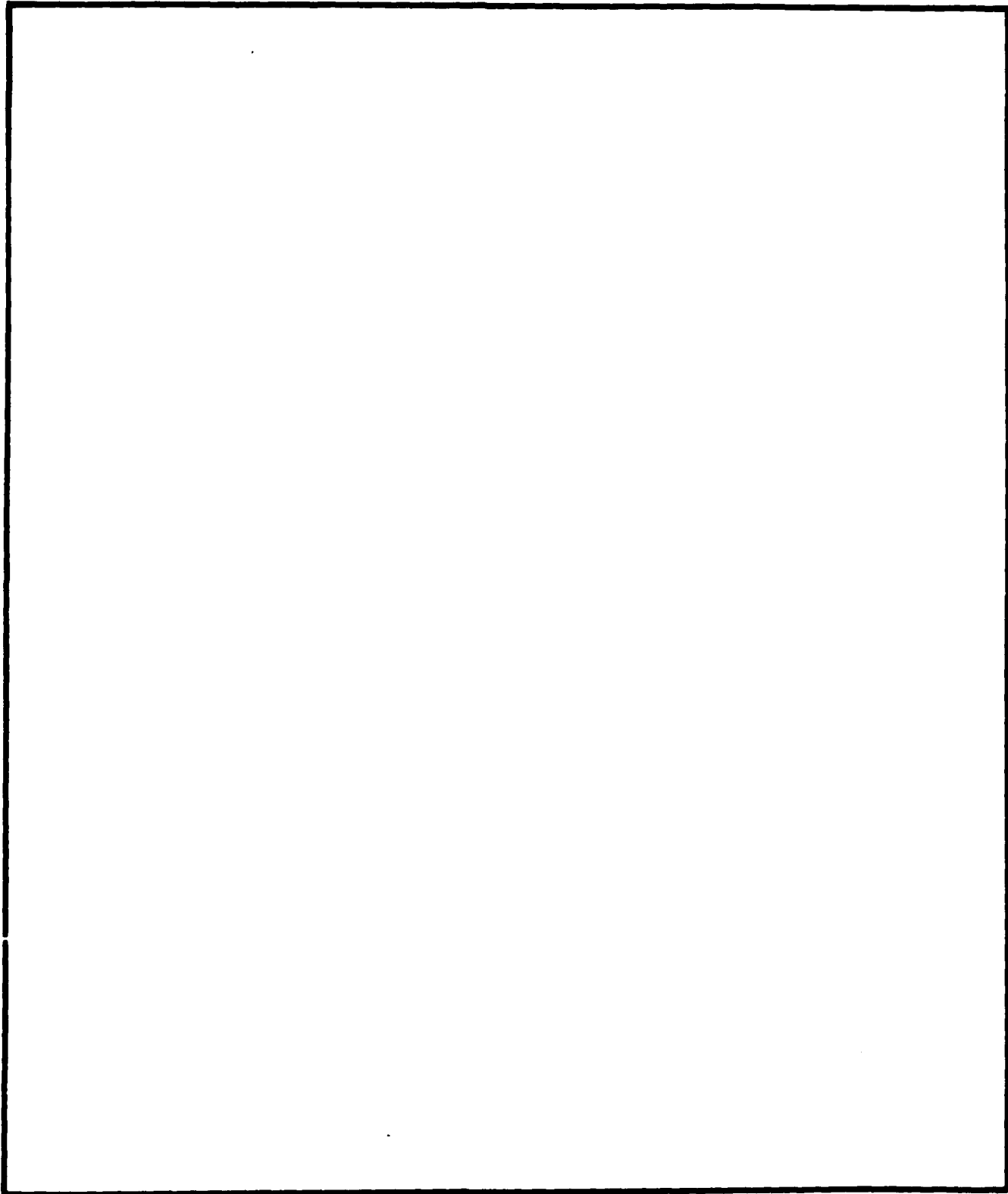
Previous editions are obsolete

S/N 0102-LF-014-6603

SECURITY CLASSIFICATION OF THIS PAGE

UNCLASSIFIED

SECURITY CLASSIFICATION OF THIS PAGE



NADC-88141-60 (Volume I)

CONTENTS

	Page
FIGURES	v
TABLES	vi
FOREWORD	vii
INTRODUCTION	1
TEST SPECIMENS AND APPARATUS	4
Experimental Setup	6
Possible Errors in X-ray Stresses	11
MEASUREMENTS ON TITANIUM	13
MEASUREMENTS ON ALUMINUM	19
Additional Results for Aluminum	19
Discussion of the Aluminum Results	23
MEASUREMENTS ON TITANIUM UNDER LOAD	26
Static Loading	26
Repeat Measurements Under Static Load	26
Cyclic Loading	33
Discussion of the Unexplained Behavior After Yielding	34
EVALUATION OF THE X-RAY SYSTEM	39
General Utility of the Equipment	39
Repeatability, Accuracy, and Precision	41
Maintenance	42
DISCUSSION AND PLANS	45
CONCLUSIONS	46
REFERENCES	47
APPENDIX A: Paper by Dowling, Hendricks, and Ranganathan on "Residual Stress Measurements in Notched Test Specimens Using X-Ray Diffraction"	A-1



Accession For	
NTIS CRA&I	<input checked="" type="checkbox"/>
DTIC TAB	<input type="checkbox"/>
Unannounced	<input type="checkbox"/>
Justification	
By	
Distribution/	
Availability Codes	
Dist	Avail and/or Special
A-1	

NADC-88141-60 (Volume I)

FIGURES

	Page
1 — Residual stress measurements by x-ray diffraction. (Adapted from Ref. 1).....	5
2 — Arrangement of specimen, fixtures, and x-ray source, for measurements during mechanical testing	7
3 — Notched x-ray specimen geometry.....	8
4 — Unnotched x-ray specimen geometry	9
5 — Details of the special sample alignment plate.....	10
6 — Variation of intensity of diffracted x-rays with tilt angle ψ for a large number of measurements on the titanium alloy	15
7 — Variation of diffraction peak width with tilt angle ψ for a large number of measurements on the titanium alloy	16
8 — Variation of lattice spacing with $\sin^2 \psi$ for a large number of measurements on the titanium alloy	17
9 — Variation of intensity of diffracted x-rays with tilt angle ψ for a large number of measurements on the aluminum alloy	20
10 — Variation of diffraction peak width with tilt angle ψ for a large number of measurements on the aluminum alloy	21
11 — Variation of lattice spacing with $\sin^2 \psi$ for a large number of measurements on the aluminum alloy	22
12 — Unusual diffraction peak shapes, and rapid changes in peak shape with small (1°) changes in ψ , for the aluminum alloy	25
13 — Stresses measured by x-ray diffraction during monotonic loading of an unnotched electropolished titanium specimen. The dashed line corresponds to perfect agreement with the applied stress	27
14 — Lattice spacing, d , versus $\sin^2 \psi$ data, and straight line slope giving the x-ray stress, at a load of 1.0 kip ($P/A = 9.2$ ksi) during monotonic loading of an unnotched electropolished titanium specimen.....	28
15 — Lattice spacing, d , versus $\sin^2 \psi$ data, and straight line slope giving the x-ray stress, at a load of 8.0 kip ($P/A = 73.3$ ksi) during monotonic loading of an unnotched electropolished titanium specimen.....	29
16 — Stresses measured by x-ray diffraction during four cycles of zero-to-maximum loading of a notched electropolished titanium specimen. The maximum load is 12.0 kips ($P/A = 110.0$ ksi.)	35

NADC-88141-60 (Volume I)

FIGURES CON'T.

17 — Comparison of estimated local notch stress response with x-ray data error bars for the first cycle of zero-to-maximum loading of the notched specimen 36

18 — Data and fitted line for x-ray measurement of residual stress at zero load after the first cycle of zero-to-maximum loading 37

A-1 Notched and straight test specimens. (The second notch geometry is the same as the one shown except that the notch radius is half as large.) A-5

A-2 Arrangement of specimen, fixtures, and x-ray source, for measurements during mechanical testing A-6

A-3 Test specimen mounted on alignment fixture A-7

A-4 Notch geometry A-10

A-5 Lattice spacing vs. $\sin^2\psi$ for straight titanium specimen no. T1SO2 with a machined surface A-13

A-6 Lattice spacing vs. $\sin^2\psi$ for notched aluminum specimen no. AX23 with an electro-polished surface A-14

NADC-88141-60 (Volume I)

TABLES

	Page
Table 1 — Materials identification and properties	3
Table 2 — Setup parameters for measurements at 1° increments in ψ	14
Table 3 — Repeat measurements on an unnotched, electropolished specimen, no. T1SO6 of Ti-6Al-4V, while under load	31
Table A-1 — Equipment parameters	A-12
Table A-2 — Experimental results	A-16

NADC-88141-60 (Volume I)

FOREWORD

The work described in this report was performed by the Virginia Polytechnic Institute and State University, Engineering Science and Mechanics Department, for the Naval Air Development Center under contract number N62269-85-C-0256. The principal investigator was Prof. Norman E. Dowling. DeRome O. Dunn, Graduate Research Assistant, performed important portions of the work. Volume II was taken from a M. S. thesis written by K. Ranganathan. The program manager for NADC was L. W. Gause; the project engineer was R.E. Vining. This interim report covers work that was performed during the time period October 1985 to December 1987.

NADC-88141-60 (Volume I)

INTRODUCTION

This interim report describes work on a three year project on Residual Stress Changes in Fatigue. It is scheduled for completion in September 1988. The project's objective is to aid the Naval Air Development Center predict and improve durability of aircraft structures.

The specific work involves modeling cycle and time dependent relaxation of residual stresses and incorporation of this model into a computer program for fatigue life prediction. A local stress-strain approach is being used to handle geometries containing stress raisers (notches), and an important part of the work is the verification of the model by direct measurement of residual stresses in notches by x-ray diffraction.

This interim report describes the work done so far which is related specifically to x-ray diffraction measurements. Some progress has also been made in the stress-strain modeling area, but this will be reported later when it is more complete.

In the remainder of this report, the experimental setup which is being used to make residual stress measurements during brief pauses in fatigue tests, is described. The Appendix gives a detailed description of the X-ray stress measuring apparatus. A detailed analytical study of various possible sources of error in the measurements is given in Volume II of this report. Data and discussion are then given which are specific to the two materials under study, namely the metal alloys Ti-6Al-4V and 7475-T651 Al. (These materials are identified, and mechanical properties given, in Table 1.) Measurements which have been obtained for titanium during static and cyclic loading

NADC-88141-60 (Volume I)

are discussed next. Following this, an evaluation of the x-ray system is presented. Finally, some general discussion and plans for future work are given, followed by appropriate conclusions.

NADC-88141-60 (Volume I)

Table 1 - Materials identification and properties

	<u>Ti-6Al-4V</u>	<u>7475-T651 Al</u>
Form	3/8 in. plate	3/4 in. plate
Condition	Mill annealed 1450°F	Solution treated and aged
Identification	Ingo ⁺ No: 990211-02-00	Serial No: 511348-1
Source	RMI, Niles, OH	Alcoa Labs, Alcoa Ctr., PA
Ultimate, ksi	142	78*
Yield, 0.2%, ksi	133	67*
Elongation, %	14	9*

* Property minimums from Metals Handbook; not test data.

NADC-88141-60 (Volume I)

TEST SPECIMENS AND APPARATUS

The x-ray diffraction method determines stresses from measuring the spacing of crystal lattice planes. Lattice spacings give elastic strains, which are related to stresses by the theory of elasticity.

Figure 1 illustrates the procedure. Monochromatic x-ray radiation diffracts according to Bragg's law:

$$n\lambda = 2d\sin\theta \quad (1)$$

where λ is the wavelength, n is the order of reflection, d is the spacing between the particular crystal lattice planes that have been chosen for observation, and 2θ is the diffraction angle as defined in Fig. 1. In Fig. 1a, the incidence angle, α , and the exit angle, β , are equal to each other and to θ . The x-ray detector then measures the intensity of radiation which is diffracted from planes parallel to the sample surface. Plotting this intensity as a function of small variations in 2θ yields a diffraction peak. The 2θ position of this peak used in Eq. 1 yields the lattice spacing for this normal orientation, called d_n .

The angle between the x-ray source and the sample is then changed by an amount ψ , called the tilt angle, giving the situation shown in Fig. 1b. Diffraction now occurs from lattice planes that make an angle ψ relative to the sample surface. If there is a surface stress in the sample, the diffraction peak will now be shifted due to different strains, hence different lattice spacings, in the new orientation. The new 2θ position of the peak used in Eq. 1 gives the new lattice spacing, d_ψ .

The stress, σ , is then determined from the relationship [2]:

$$\sigma = \frac{E}{(1+\nu)} \frac{1}{\sin^2\psi} \frac{(d_\psi - d_n)}{d_n} \quad (2)$$

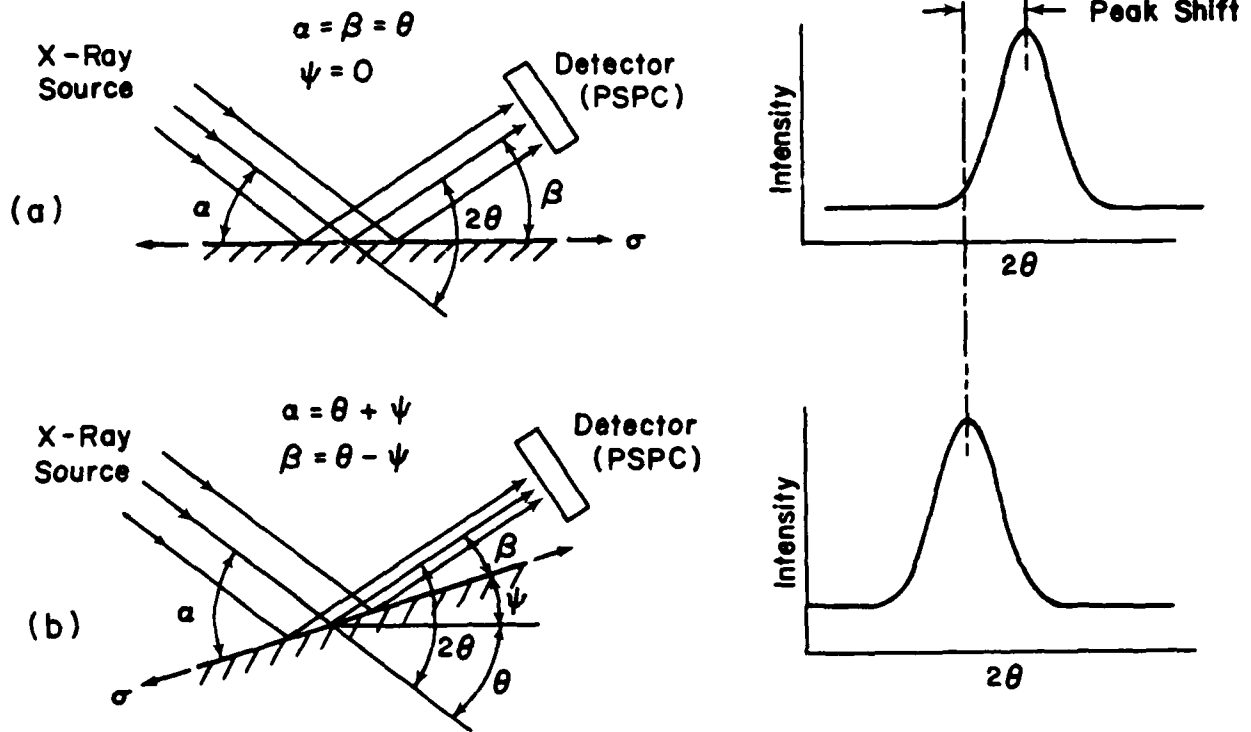


Fig. 1 - Residual stress measurements by x-ray diffraction. (Adapted from Ref. 1).

NADC-88141-60 (Volume I)

where E and ν are Young's modulus and Poisson's ratio, respectively, for the chosen crystallographic planes. In practice, diffraction peaks are obtained for several values of ψ , and the stress is determined from Eq. 2 and the slope of data points on a plot of d_{ψ} versus $\sin^2\psi$.

Experimental Setup

In the present work, such measurements are being made using a TEC series 1600 x-ray diffraction system on loan from the U.S. Navy and located at Virginia Polytechnic. The variation of tilt angle, ψ , is accomplished by the automated motion of the x-ray source and detector, while the sample remains stationary. This allows measurements to be made on a test specimen during brief pauses in a fatigue test as illustrated in Fig. 2.

Notched test specimens as shown in detail in Fig. 3 can be studied. These have a notch root radius of either 0.25 or 0.125 in., which give stress concentration factors of 1.61 and 2.02, respectively. Unnotched specimens as in Fig. 4 are used to verify the x-ray diffraction measurements by comparison with the known applied stress. For both materials the long axis of the specimen is parallel to the rolling direction of the original plate of material, and the specimen thickness is parallel to the plate thickness.

The alignment plate indicated in Fig. 2 is shown in detail in Fig. 5. A corresponding part of the TEC system is disassembled and replaced with this plate, which "locks on" to the specimen to assure its proper alignment and positioning for the measurement.

Additional detail on the experimental setup is given in Appendix A. The time required to obtain an x-ray stress measurement is found to

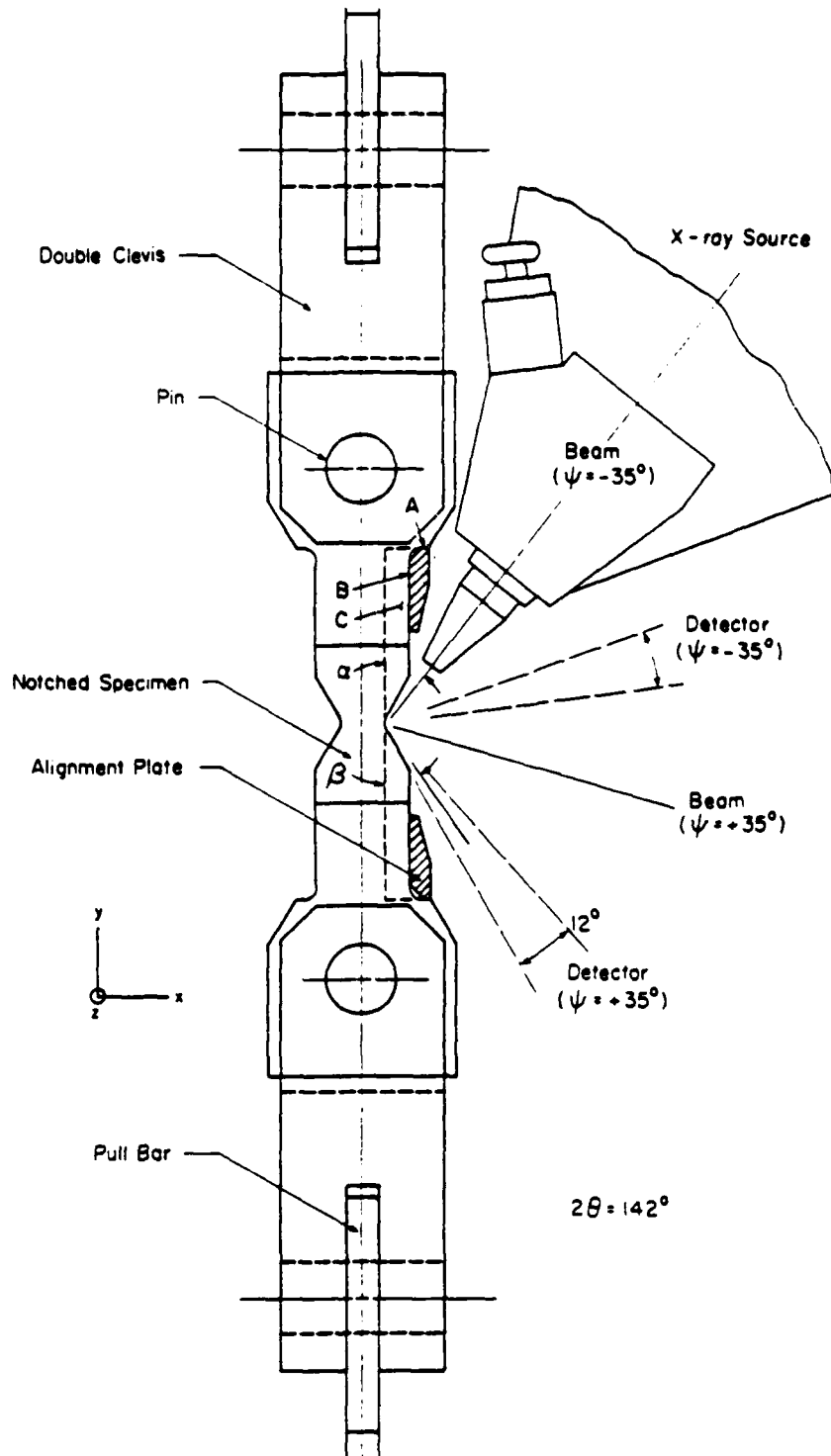
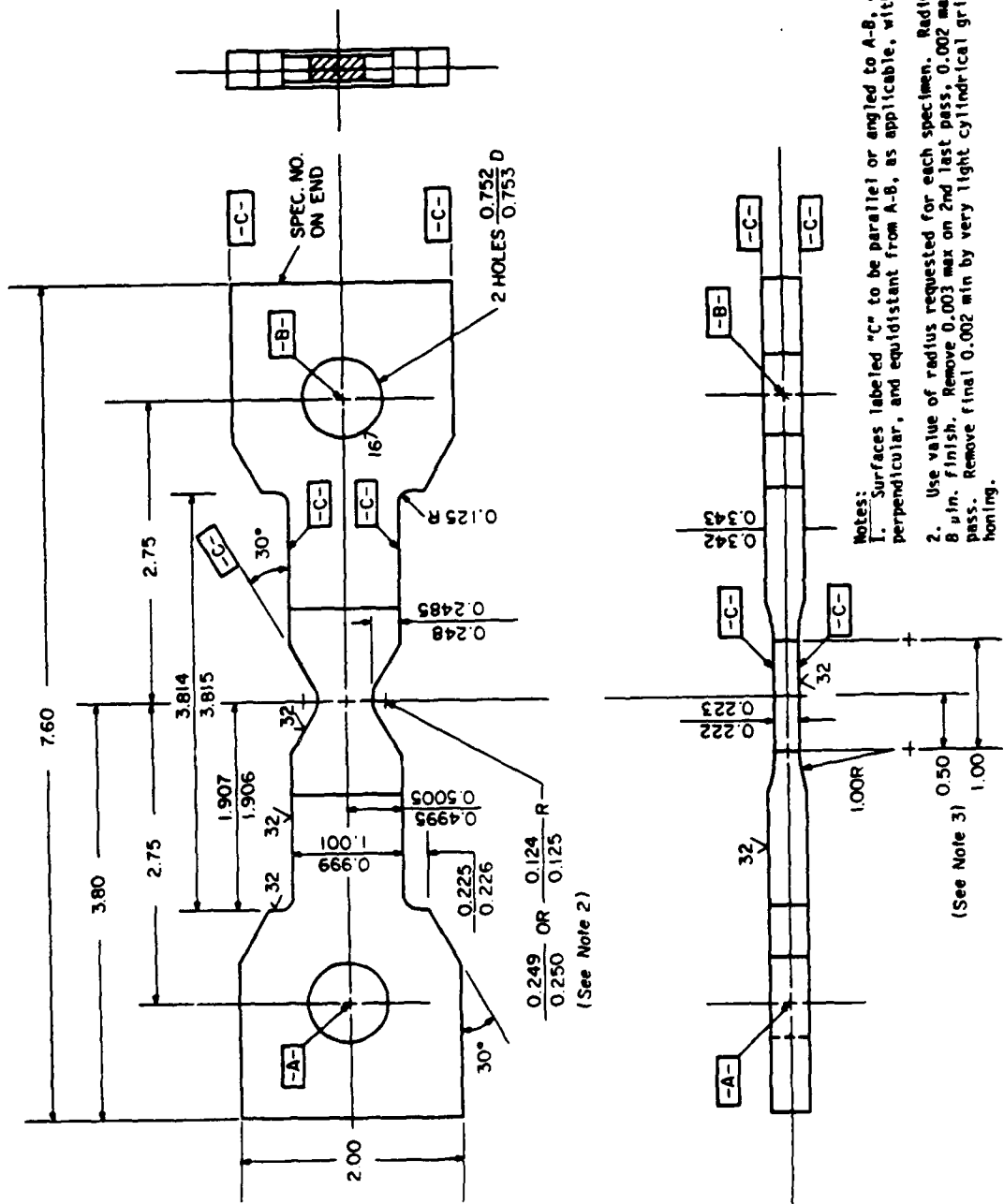


Fig. 2 - Arrangement of specimen, fixtures, and x-ray source, for measurements during mechanical testing.



Notes:
 1. Surfaces labeled "C" to be parallel or angled to A-B, and mutually perpendicular, and equidistant from A-B, as applicable, with 0.001.

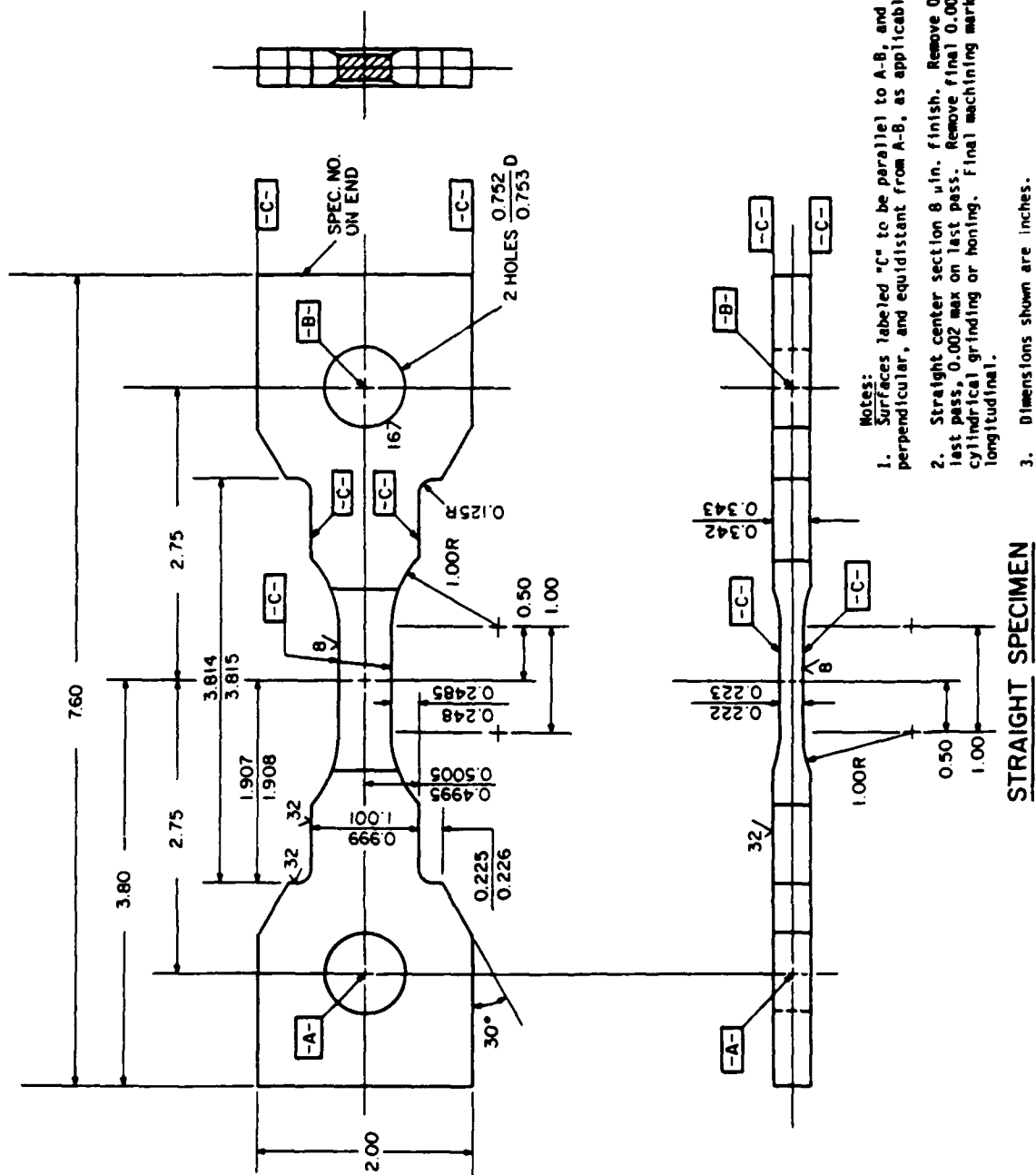
2. Use value of radius requested for each specimen. Radius 8 in. Finish. Remove 0.003 max on 2nd last pass, 0.002 max on last pass. Remove final 0.002 min by very light cylindrical grinding or honing.

- 3. Dimensions to tangency of 1.00R
- 4. Dimensions shown are inches.

X-RAY SPECIMEN

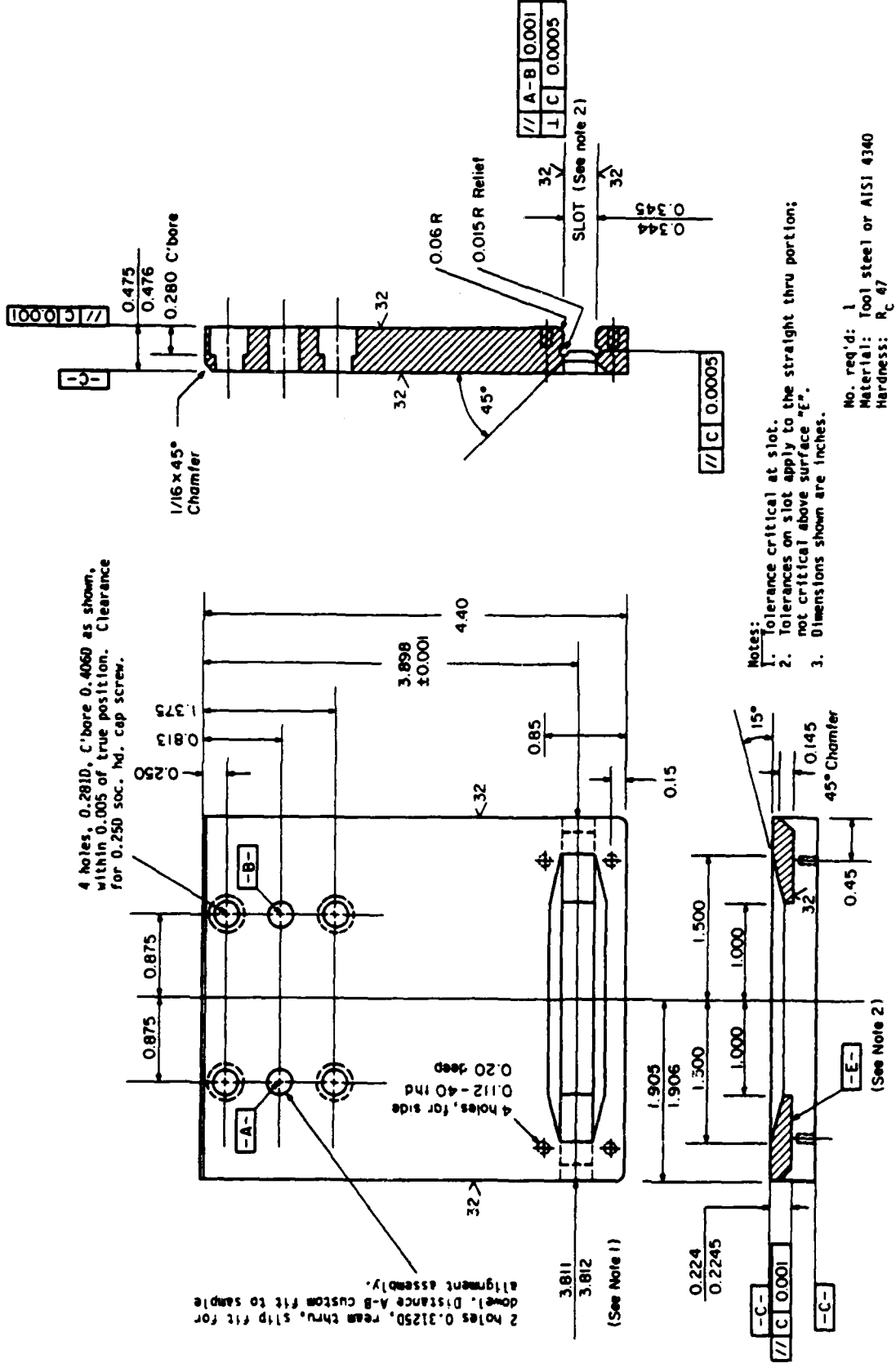
(See Note 3)

Fig. 3 - Notched x-ray specimen geometry.



- Notes:
1. Surfaces labeled "C" to be parallel to A-B, and mutually perpendicular, and equidistant from A-B, as applicable, within 0.001.
 2. Straight center section 8 in. finish. Remove 0.003 max on 2nd last pass, 0.002 max on last pass. Remove final 0.002 min by very light cylindrical grinding or honing. Final machining marks to be longitudinal.
 3. Dimensions shown are inches.

Fig. 4 - Unnotched x-ray specimen geometry.



SPECIAL ALIGNMENT PLATE

Fig. 5 - Details of the special sample alignment plate.

NADC-88141-60 (Volume I)

be about 5 minutes for the aluminum alloy and 20 minutes for the titanium alloy.

Possible Errors in X-ray Stresses

Various sources of error in the measurements need to be considered.

Measurements are confined to a narrow strip in the bottom of the notch to avoid errors associated with the decrease in stress around the radius of the notch and other geometric effects of the radius. For the blunter notch, an x-ray beam size of 1 mm by 5 mm is appropriate, with the 5 mm dimension being parallel to the specimen thickness, that is, the z-direction in Fig. 2. For the sharper notch, the beam size must be reduced to 0.5 mm x 5 mm. Use of the 5 mm beam width takes advantage of most of the specimen thickness so as to maximize the area of x-ray impingement, which in turn minimizes the measurement time and minimizes difficulties with effects due to the finite crystallographic grain size of the material.

Detailed analysis of the stress distribution and gradients in the notched specimen and of various possible errors are given in Volume II of this report.

The error due to variation of the stress around the radius of the notch is found not to exceed 1% in stress over the area impinged by x-rays at the extremes of ψ . Another concern is that the finite depth of penetration of the x-rays may be sufficient for the stress gradient in the x-direction in Fig. 2 to cause an error. This results from the measurement being based on diffracted x-rays from a volume where the stress is on the average less than the maximum (surface) value. However, for the various combinations of material, type of radiation, choice of 2θ , and range of ψ involved, this error also does not exceed 2% in stress.

NADC-88141-60 (Volume I)

There is also an error due to the curvature of the sample [3] alone. This error produces a fixed error in stress that is independent of the measured stress. The worst case of interest is the sharper notch and titanium material, where this error is still less than 2 ksi.

In addition, various effects that might cause error are corrected for in the automated data analysis of the TEC system. These include: $K_{\alpha 1} - K_{\alpha 2}$ peak splitting, Lorentz polarization, absorption variations with ψ , and finite beam geometry. The overall conclusion is reached that accurate measurements are possible on the notched specimens. This is true provided that close alignment and positioning are maintained, with the alignment plate arrangement being thought to be sufficient to handle this requirement. Of special importance is the depth of the bottom of the notch below the alignment plate, hence the distance from x-ray source to sample. This is checked for each measurement and adjusted in increments of 0.001 in. by shims if necessary.

NADC-88141-60 (Volume I)

MEASUREMENTS ON TITANIUM

Using an unnotched electropolished specimen, large number of diffraction peaks were obtained at 1° increments over a wide range of relative tilt angles, ψ , specifically over $\psi = \pm 35^\circ$. Setup parameters for these measurements are given in Table 2. The intensity of each diffraction peak plotted versus ψ in Fig. 6, where the intensity is a relative measure of the number of photons counted per unit time during the sample period. The two symbol (+ versus x) correspond to rotating the specimen 180° , that is, switching ends. A factor of two variation in intensity is observed with a minimum around $\psi = 0$.

The corresponding peak widths, specifically the full-width-at-half-maximum (FWHM) values, are plotted versus ψ in Fig. 7, and the measured lattice spacings versus $\sin^2\psi$ in Fig. 8. Peak shape at the lower intensities near $\psi = 0$ in Fig. 6 is less accurately determined since it is based on a lower photon count. Peak shape affects the FWHM and the location of the peak maximum, hence the measured lattice spacing. The extra scatter in Figs. 7 and 8 around $\psi = 0$ is partially due to this situation.

Therefore, to assure a reasonable signal-above-background, it was decided to subsequently make x-ray stress measurements by avoiding ψ in the range $\pm 12^\circ$. This decreases the range of $\sin^2\psi$ available for fitting using Eq. 2, but the accuracy of the measurements is improved overall by making this compromise and avoiding the large scatter near $\psi = 0$.

The intensity variations of Fig. 6 indicate a minor degree of preferred orientation, but not enough to seriously impair the ability to make x-ray stress measurements. This conclusion is supported by the

NADC-88141-60 (Volume I)

Table 2 - Setup parameters for measurements at 1° increments in ψ ¹

Material	Ti-6-4	7475 A1	7475 A1	7475 A1
Radiation	Cu	Cu	Cr	Cu
Diff. angle, 2 θ , deg.	142°	160°	142°	142°
Diff. planes, (hkl)	(213)	(511)/(333)	(311)	(422)
Spec. no.	T1S06	AS12	AS12	AS12
Data file nos.	109-112 114-125	140-154 (155-171) ²	195-200 203-210	172-187
Range of ψ , deg.	-35 to +35	-33 to +44	-33 to +35	-33 to +44
ψ osc. range, deg.	0	0	0	0
Slit size, mm x mm	1 x 5	0.5 x 5 (3 x 5) ²	0.5 x 5	0.5 x 5
Counting time, sec.	180	70 (20) ²	460	210

Notes:

¹ Electropolished specimens under zero load. All measurements were repeated after switching ends of the specimen.

² The measurements for all 1° increments were repeated using the setup parameters in parenthesis.

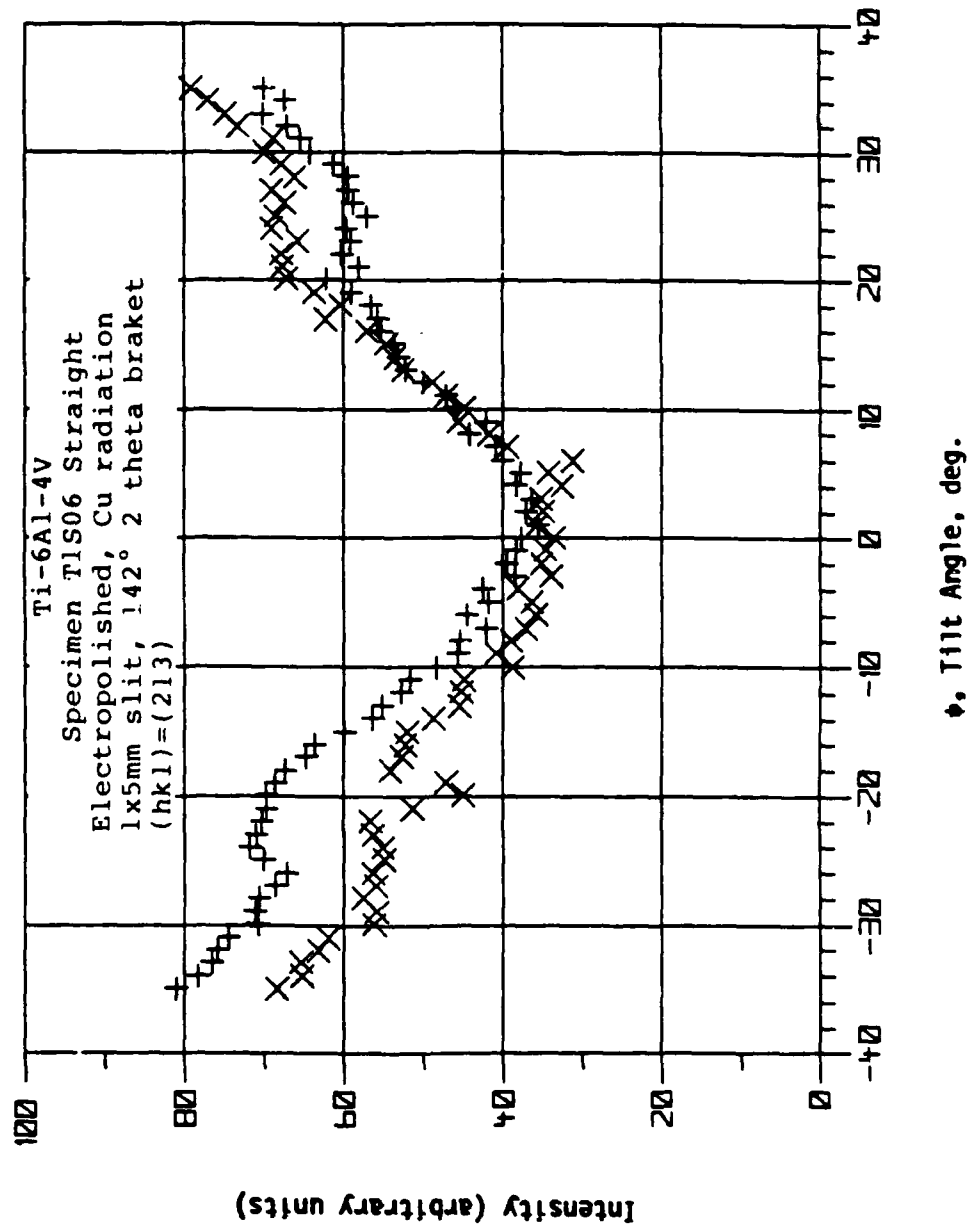


Fig. 6 - Variation of intensity of diffracted x-rays with tilt angle ψ for a large number of measurements on the titanium alloy.

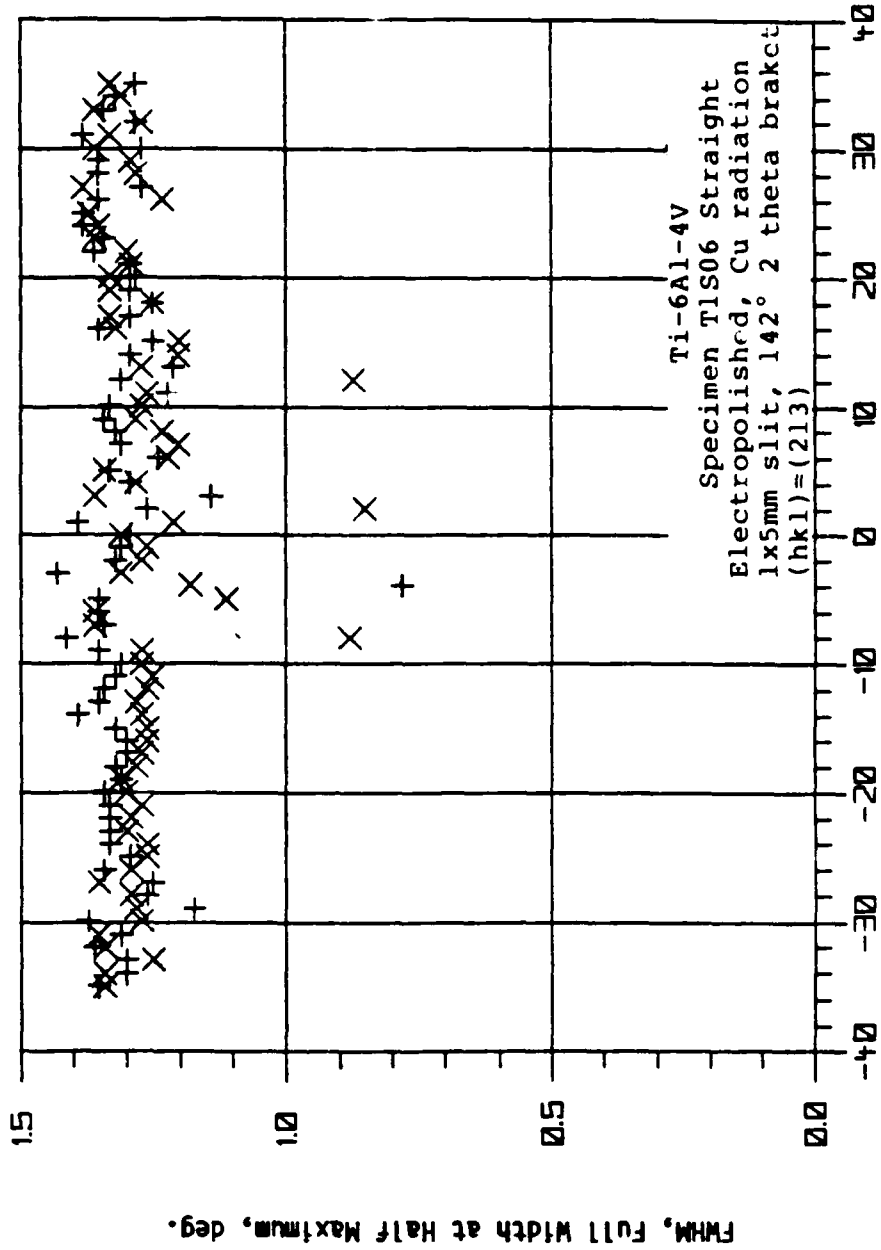


Fig. 7 - Variation of diffraction peak width with tilt angle ψ for a large number of measurements on titanium alloy.

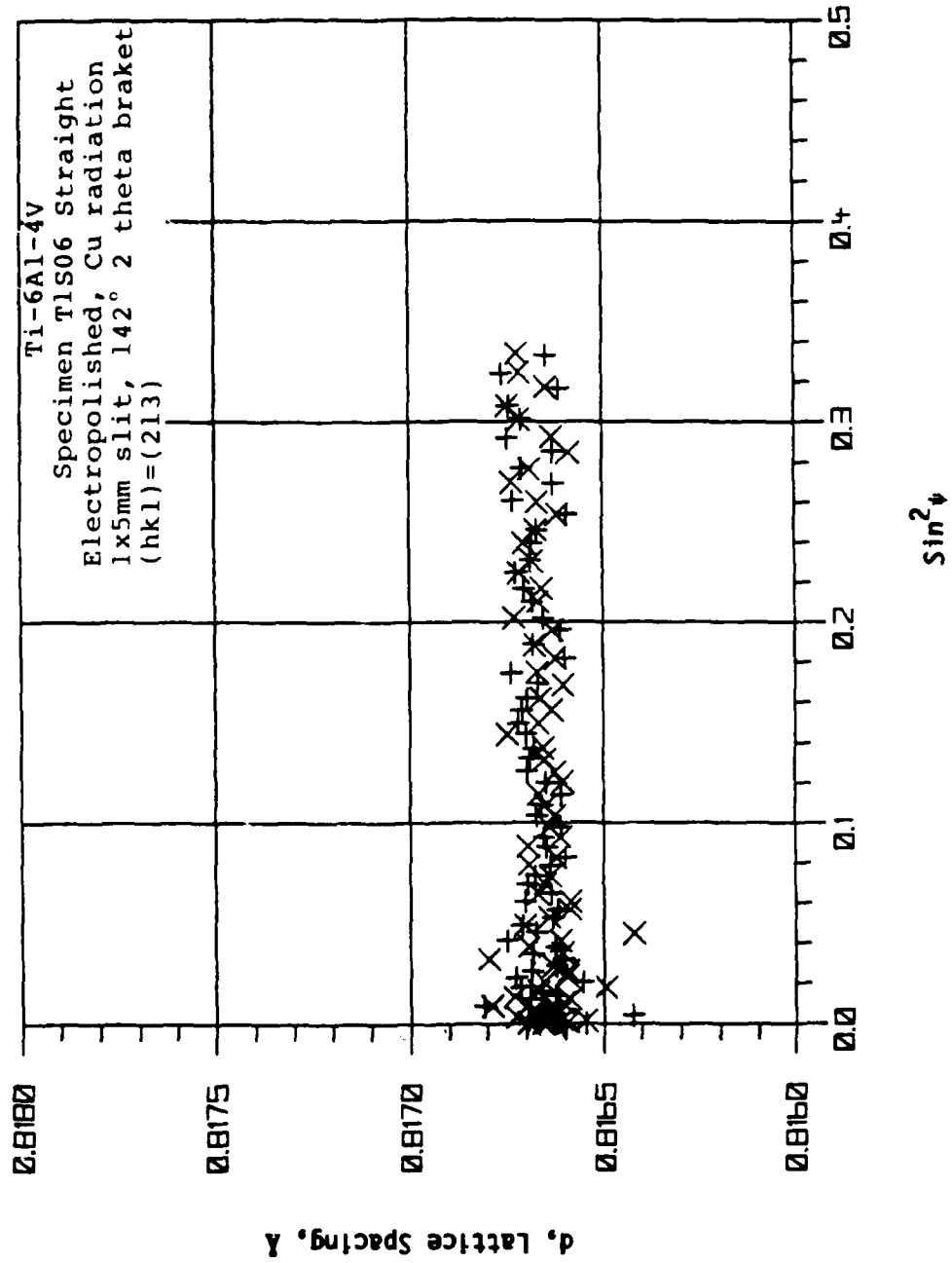


Fig. 8 - Variation of lattice spacing with $\sin^2\psi$ for a large number of measurements on the titanium alloy.

NADC-88141-60 (Volume I)

fairly constant FWHM, excepting of course the scatter around $\psi = 0$.
And it is further supported by the linear trend of the lattice spacing data of Fig. 8. The zero slope of this data trend is consistent with the expectation of nearly zero residual stress in the sample due to electropolishing.

NADC-88141-60 (Volume I)

MEASUREMENTS ON ALUMINUM

Similar measurements of a large number of diffraction peaks were made on a single unnotched, electropolished specimen of 7475-T651 Al. Intensity and FWHM versus ψ , and lattice spacing versus $\sin^2\psi$, are shown in Figs. 9-11 for the case of Cu radiation, $2\theta = 160^\circ$, and slit size 0.5×5 mm. Setup parameters are given in the second column of Table 2. For the plot of lattice spacing, d , versus $\sin^2\psi$, the plot covers the same size window in d as does Fig. 8 for titanium so that the scatter can be compared.

In contrast to the titanium results, the intensity varies widely over more than a factor of thirty, and the FWHM varies considerably and erratically with ψ . Also, the lattice spacing versus $\sin^2\psi$ does not exhibit a linear trend, and has considerable scatter, so that no well-defined slope exists from which to determine a stress using Eq. 2.

Additional Results for Aluminum

The experiments were then repeated except that the slit size was increased to 3×5 mm. Setup parameters were the same as before except as indicated in parenthesis in the second column of Table 2. In these results (not shown) the intensity variation was similar or perhaps even greater, the FWHM scattered even more, and the lattice spacing showed a similar trend.

In an attempt to find a set of diffracting planes for which successful stress measurements could be made, two additional sets of data similar to Figs. 6-8 were obtained using the 0.5×5 mm slit. These corresponded to Cr radiation at $2\theta = 142^\circ$, where the diffracting planes are $(hkl) = (311)$, and to Cu radiation at $2\theta = 142^\circ$, where the

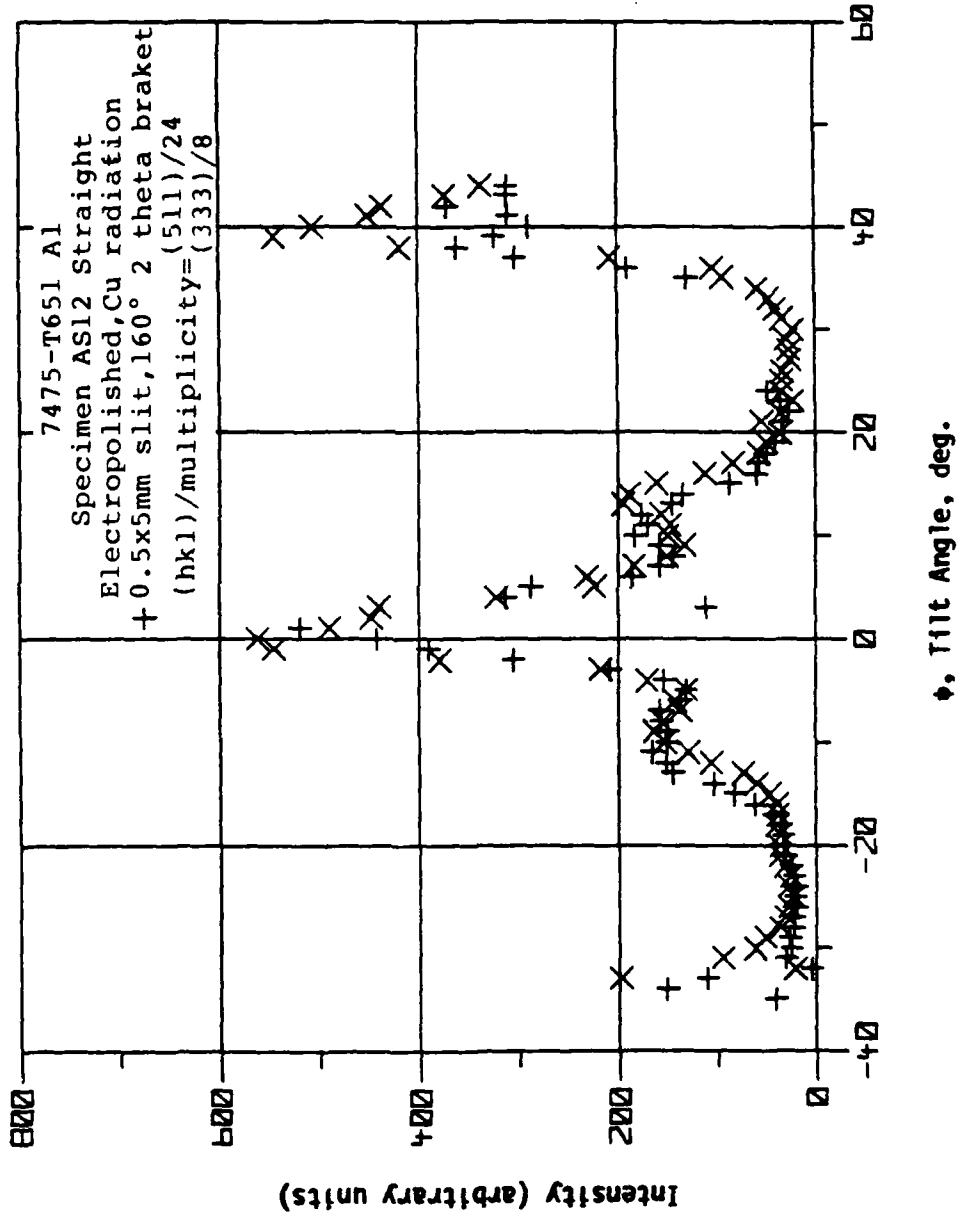


Fig. 9 - Variation of intensity of diffracted x-rays with tilt angle ϕ for a large number of measurements on the aluminum alloy.

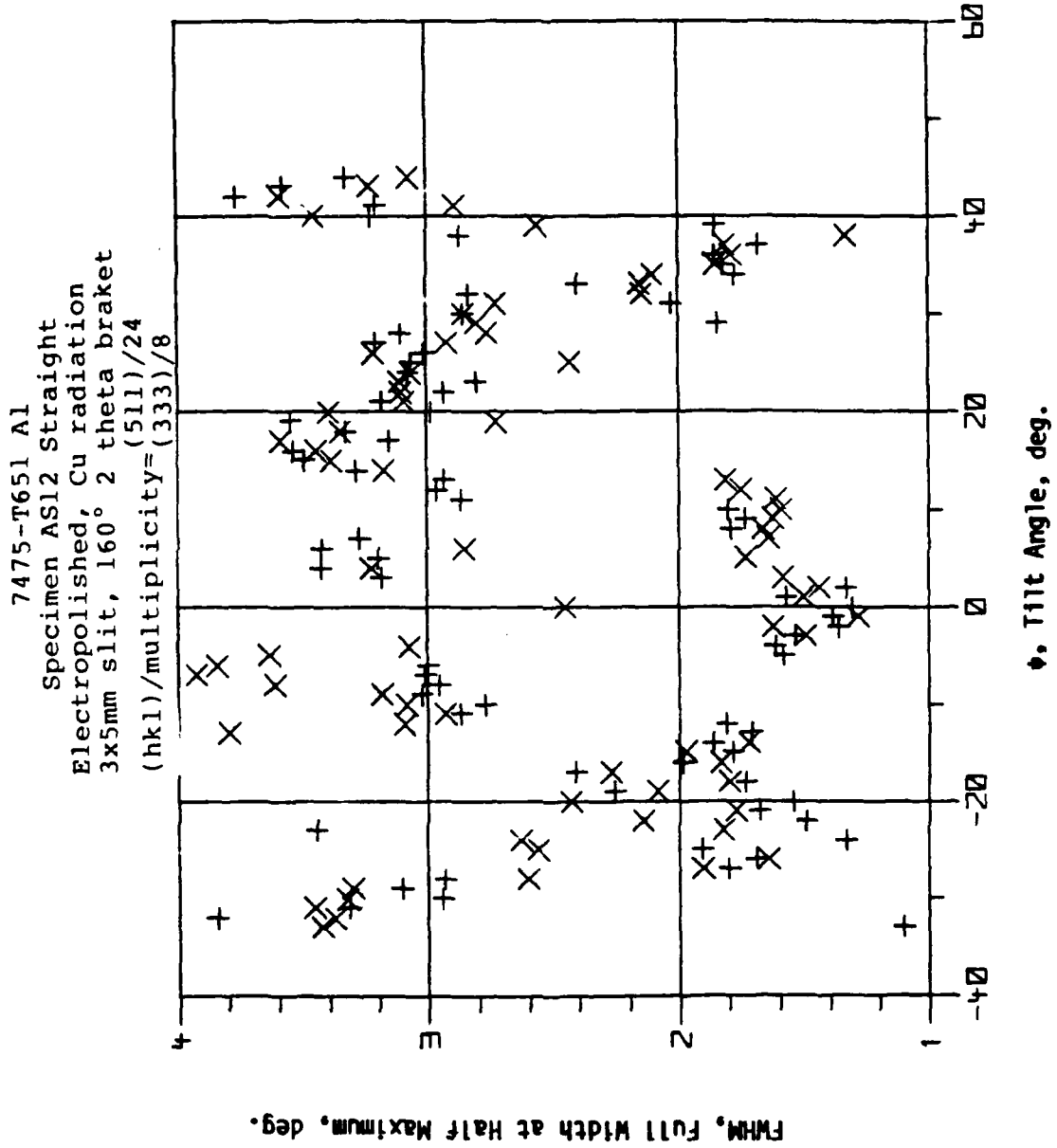


Fig. 10 - Variation of diffraction peak width with tilt angle ψ for a large number of measurements on aluminum alloy.

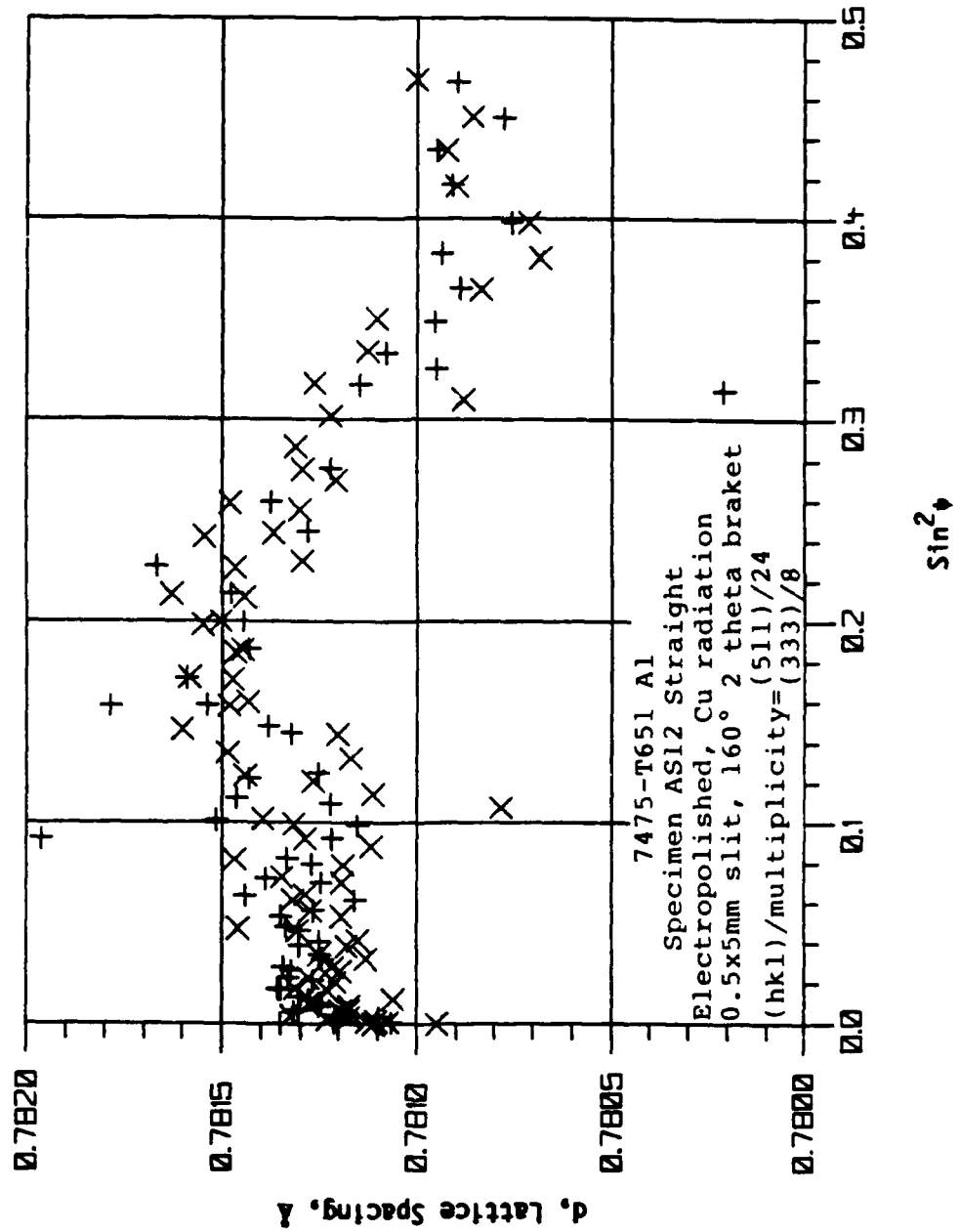


Fig. 11 - Variation of lattice spacing with $\sin^2\psi$ for a large number of measurements on the aluminum alloy.

NADC-88141-60 (Volume I)

planes are $(hkl) = (422)$. Setup parameters are given by the last two columns of Table 2.

However, large intensity variations occurred in both cases. For the Cr/142° on aluminum case, the FWHM varied by an amount similar to that for Cu/142° on titanium. But the FWHM was again large for the Cu/142° on aluminum case. In both cases the lattice spacing data exhibited large scatter and no clear linear trend. Hence, neither of these additional sets of planes can be used to obtain suitable stress measurements in the usual manner.

Discussion of the Aluminum Results

If the difficulty were caused by large grain (or other particle) size, increasing the slit area by a factor of 6 for the Cu/160° combination should have had a beneficial effect. Also, the grain size has been determined to be quite fine, in the range 10-15 μm . The difficulty therefore appears to be associated with preferred grain orientation, that is, texture. This situation was later confirmed by a pole figure done on this material by Lambda Research, Inc., Cincinnati, OH.

It is interesting to note that preliminary study of the aluminum material did not indicate that the preferred orientation problem was particularly severe. (See Appendix). This occurred because the small number of ψ angles chosen for study fortuitously resulted in most cases in a lattice spacing plot that looked reasonable, and even in a straight line fit for the stress value with reasonable statistics. One can thus be "fooled" into thinking a measurement is good when the result is influenced by preferred orientation.

An additional indicator of preferred orientation is that the

NADC-88141-60 (Volume I)

diffraction peak shapes are irregular and vary rapidly with small changes in ψ . This is illustrated in Fig. 12 for the same case as for Figs. 9-12, that is Cu/160° with 0.5 x 5 mm slit. The three peaks shown differ markedly, despite being separated by only 1° in ψ . A variety of such peaks were examined, and various odd shapes were seen, such as double peaks, very wide peaks, and indistinct peaks. Of course, peak shift data resulting from forced fits to such odd peaks have little meaning, and neither do the resulting x-ray stress values.

The particular situation of double peaks, or peak splitting, is thought to be due to the (511) and (333) planes having relative intensities that change with diffraction orientation. Under normal circumstances, the (511) diffraction would be dominant due to the multiplicity of these planes being three times greater than for the (333) planes. However, the preferred orientation may cause the (333) planes to sometimes dominate, and to have slightly different peak shifts than the (511) planes, and since the two cannot be separated, peak shift measurements are confounded. Such preferred orientation is not a generic situation in 7475 Al, as at least one batch of material has been recently located that does not exhibit such behavior. It is not clear at this point whether the degree of preferred orientation in this batch of 7475 Al is unusual, or whether similar situations will frequently occur in working with this and similar materials.

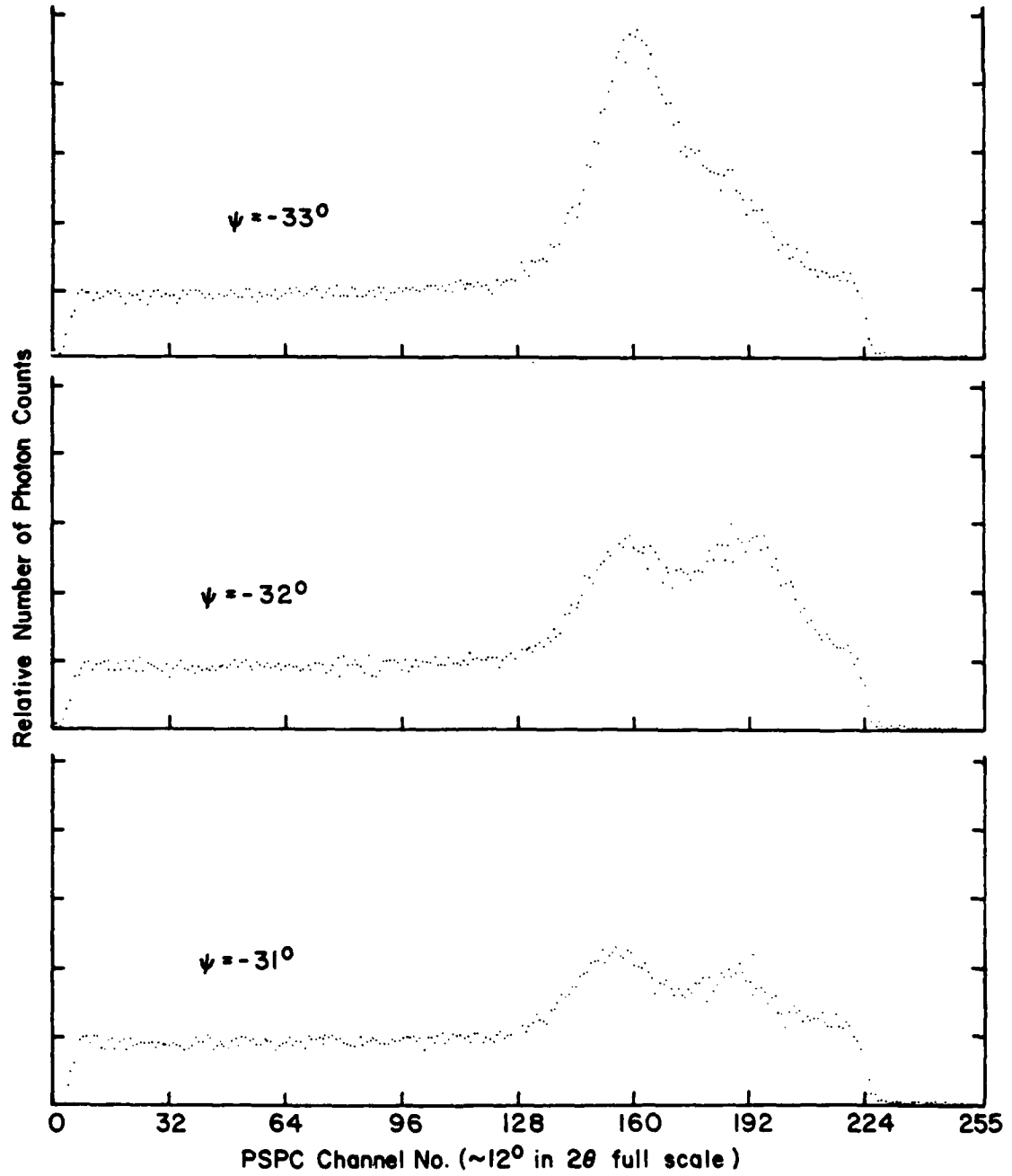


Fig. 12 - Unusual diffraction peak shapes, and rapid changes in peak shape with small (1°) changes in ψ , for the aluminum alloy.

NADC-88141-60 (Volume I)

MEASUREMENTS ON TITANIUM UNDER LOAD

Electropolished specimens of Ti-6Al-4V were studied during static and cyclic loading by making x-ray stress measurements with the specimen temporarily held at various values of load.

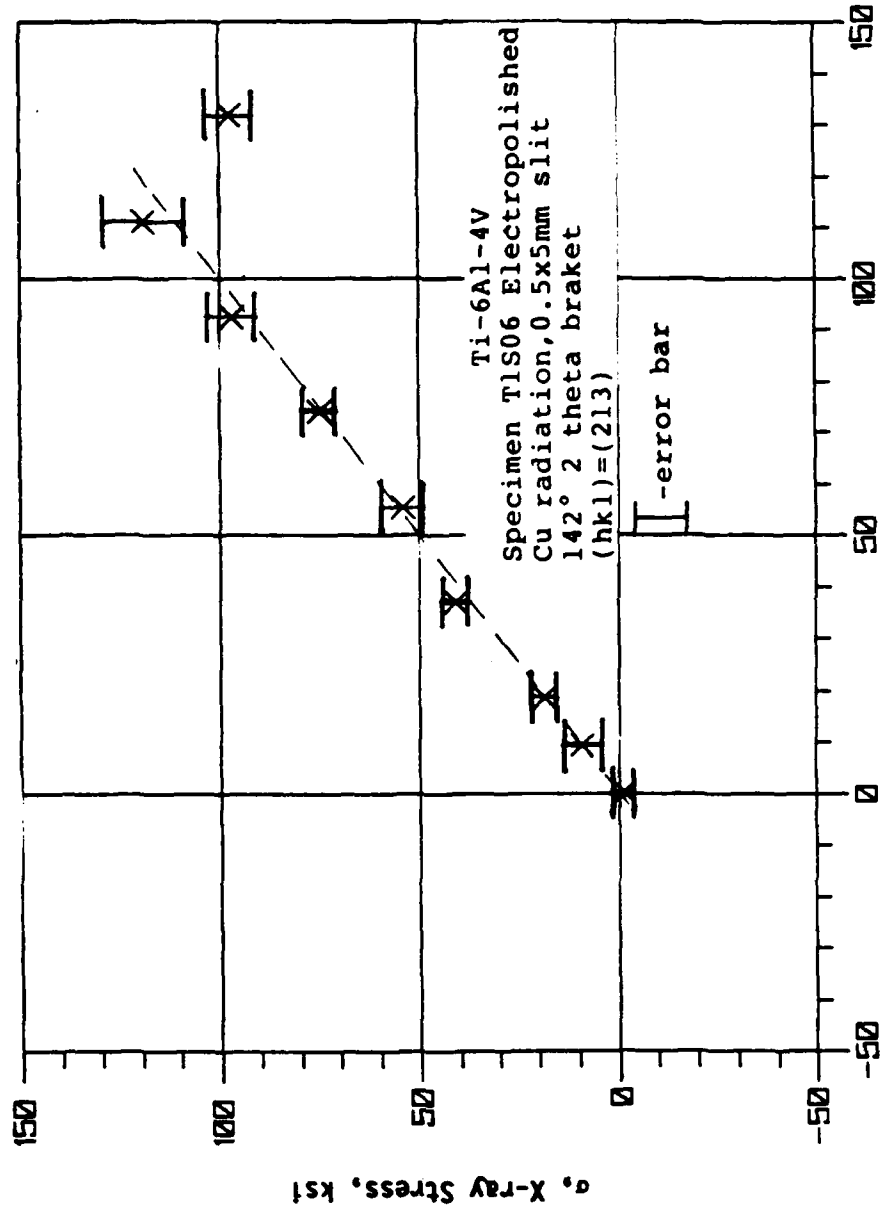
Static Loading

Data of x-ray stress versus applied stress for static loading of an unnotched specimen are shown in Fig. 13. Two of the lattice spacing plots, the slopes of which give the x-ray stress using Eq. 2, are given as Figs. 14 and 15. In Fig. 13, there is excellent agreement between x-ray and applied stresses, as indicated by the dashed line, until yielding occurs. Yielding begins at a proportional limit around 123 ksi, and the 0.2% offset yield strength is about 140 ksi. (The test specimens appear to have slightly higher yield strengths than the mill test reports on this plate of material, which are the source of the values in Table 1.)

Beyond yielding, the x-ray stress decreases while the applied stress continues to increase. In principle, the presence of plastic strain should not affect the stress measurements, as this depends on only the elastic portion of the strain, which is expected to still obey Hooke's Law.

Repeat Measurements Under Static Load

During the static loading work just described, repetitive measurements were made, and some of the experimental parameters were varied in an attempt to optimize the measurement time. This was done at three different load levels corresponding to applied stresses of 9.2, 36.7, and 73.3 ksi. Results are given in Table 3. Two of these



S = P/A, Applied Stress, ksi

Fig. 13 - Stresses measured by x-ray diffraction during monotonic loading of an unnotched electropolished titanium specimen. The dashed line corresponds to perfect agreement with the applied stress.

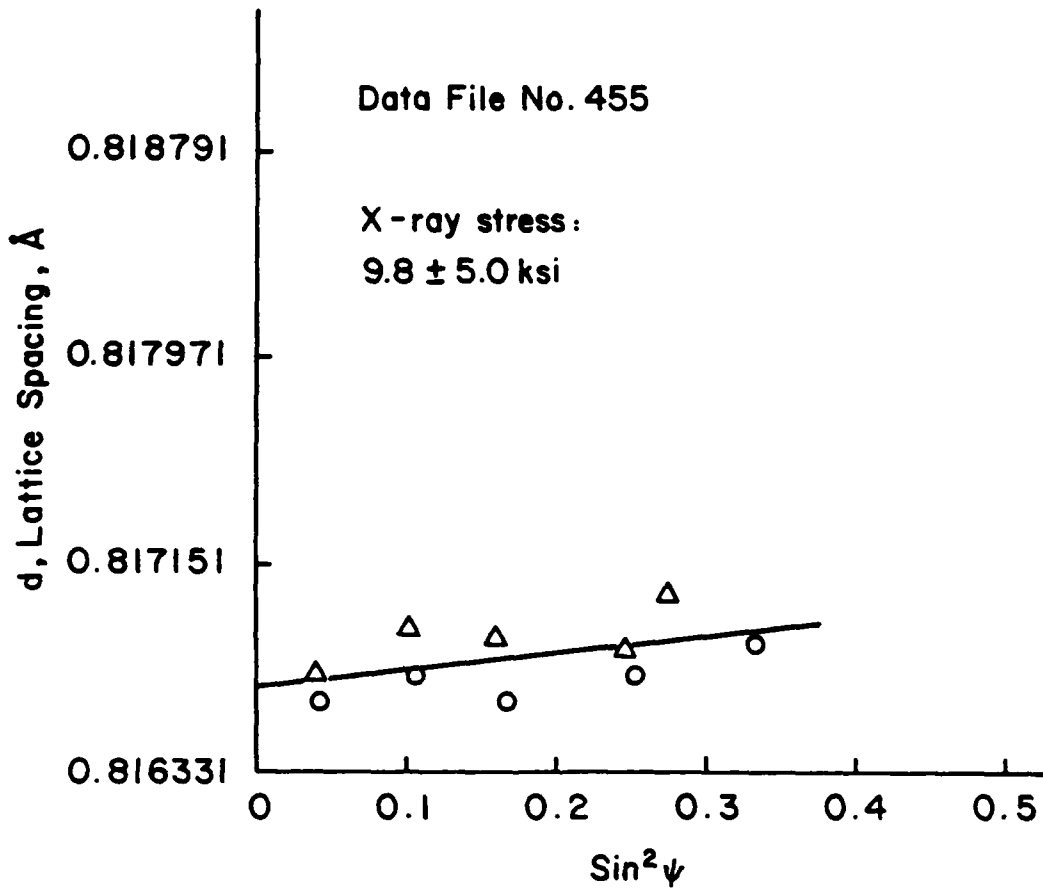


Fig. 14 - Lattice spacing, d , versus $\sin^2 \psi$ data, and straight line slope giving the x-ray stress, at a load of 1.0 kip ($P/A = 9.2$ ksi) during monotonic loading of an unnotched electropolished titanium specimen.

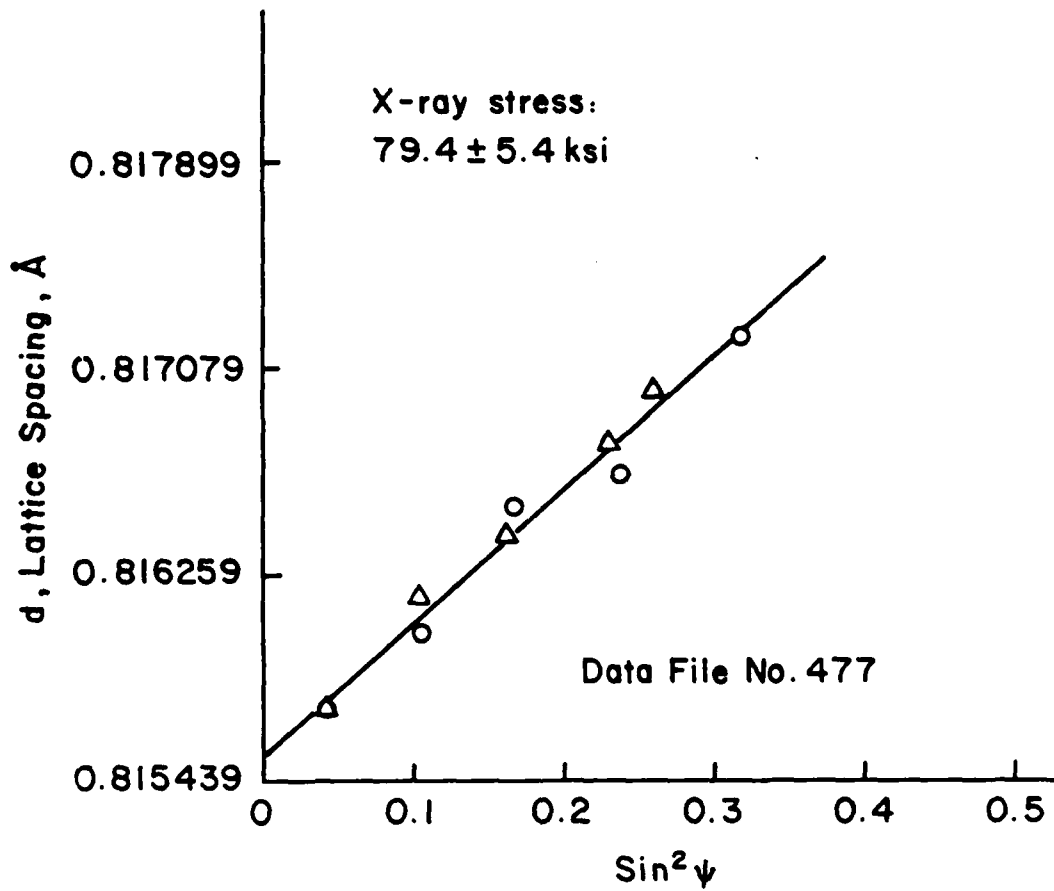


Fig. 15 - Lattice spacing, d , versus $\sin^2\psi$ data, and straight line slope giving the x-ray stress, at a load of 8.0 kip ($P/A = 73.3$ ksi) during monotonic loading of an unnotched electropolished titanium specimen.

NADC-88141-60 (Volume I)

measurements correspond to the lattice spacing plots of Figs. 14 and 15; note the corresponding "data file nos."

X-ray stress values and two types of (one standard deviation) error bands are given in Table 3. One of these errors is the counting statistics error, which is affected by counting time. The other is the goodness of fit for the straight line on the lattice spacing, d , versus $\sin^2\psi$ plots as in Figs. 14 and 15. The actual error is considered to be the larger of the two. If the goodness-of-fit error is significantly larger than the counting statistics error, this implies difficulty with either or both of the underlying assumptions of: 1) biaxial stress without shear in the measurement direction, and, 2) isotropic, homogenous material. For example, large goodness-of-fit errors occur for the aluminum material due to the second assumption being violated because of the preferred orientation problem, resulting in poor linearity on d versus $\sin^2\psi$ as in Fig. 11.

Errors due to finite grain size can be reduced, and the goodness of fit improved, by an automated small cyclic oscillation of the tilt angle, ψ , during measurement [4]. As indicated in Table 3, such oscillations over a range of 3° , that is $\pm 1.5^\circ$, were employed for most measurements at the two higher applied stress levels. The ψ angles investigated were all between -32 and $+35^\circ$, with values in the range $\pm 12^\circ$ being avoided as discussed earlier. Either 6 or 10 different diffraction peak measurements, each at a different ψ , were used to obtain each x-ray stress value. Where ψ oscillation was used, the extremes of ψ had to be decreased slightly to -31 and $+34^\circ$ to accommodate this.

The counting times given in Table 3 are nominal values

NADC-88141-60 (Volume I)

Table 3 - Repeat measurements on an unnotched, electropolished specimen, no. T1S06 of Ti-6Al-4V, while under load

1 kip load (P/A = 9.2 ksi)

Data file no.	450	451	452	453
Counting time, sec.	150	150	100	100
No. of ψ angles	6	6	6	6
ψ osc. range, deg.	0	0	0	0
Max. std. dev./ ψ , Å/deg.	$1.72 \times 10^{-4}/-24$	$1.00 \times 10^{-4}/-24$	$1.14 \times 10^{-4}/-12$	$6.9 \times 10^{-5}/12$
Count. stat. error, ksi	2.6	2.8	5.0	3.4
Goodness fit error, ksi	6.7	6.3	5.9	5.1
X-ray stress, ksi	12.9	12.5	11.4	10.6
FWHM, max/min, deg.	1.38/1.29	1.41/1.21	1.44/1.31	1.44/1.19
Intensity, max/min, units	33.1/21.0	31.5/20.5	32.4/20.1	32.6/20.1

1 kip load (9.2 ksi) cont'd.

Data file no.	454	455	456
Counting time, sec.	100	100	75
No. of ψ angles	10	10	10
ψ osc. range, deg.	0	0	0
Max. std. dev./ ψ , Å/deg.	$1.15 \times 10^{-4}/-32$	$1.29 \times 10^{-4}/-24$	$3.24 \times 10^{-4}/-32$
Count. stat. error, ksi	3.2	3.5	8.1
Goodness fit error, ksi	4.8	5.0	6.8
X-ray stress, ksi	9.1	9.8	11.7
FWHM, max/min, deg.	1.49/1.27	1.46/0.74	1.47/1.32
Intensity, max/min, units	29.8/21.1	31.8/19.3	33.5/19.1

NADC-88141-60 (Volume I)

Table 3 cont'd.

4 kip load (P/A = 36.7 ksi)

Data file no.	468	471	469	470
Counting time, sec.	150	150	100	100
No. of ψ angles	6	6	10	10
ψ osc. range, deg.	3	0	3	0
Max. std. dev./ ψ , Å/deg.	$7.0 \times 10^{-5}/24$	$7.8 \times 10^{-5}/-24$	$1.36 \times 10^{-4}/12$	$8.6 \times 10^{-5}/29$
Count. stat. error, ksi	2.5	3.1	4.8	3.4
Goodness fit error, ksi	3.4	6.2	4.2	5.3
X-ray stress, ksi	40.9	42.1	44.5	38.9
FWHM, max/min, deg.	1.43/1.30	1.50/1.33	1.48/1.32	1.49/1.28
Intensity, max/min, units	33.2/20.9	32.6/23.2	34.0/21.0	33.4/22.7

8 kip load (P/A = 73.3 ksi)

Data file no.	475	476	477	478
Counting time, sec.	150	150	150	150
No. of ψ angles	6	6	10	10
ψ osc. range, deg.	3	3	3	3
Max. std. dev./ ψ , Å/deg.	$8.0 \times 10^{-5}/34$	$9.0 \times 10^{-5}/-24$	$4.5 \times 10^{-4}/24$	$1.0 \times 10^{-4}/-19$
Count. stat. error, ksi	4.2	3.8	5.4	3.0
Goodness fit error, ksi	5.2	7.3	3.6	4.6
X-ray stress, ksi	70.1	76.2	79.4	78.3
FWHM, max/min, deg.	1.50/1.34	1.47/1.35	1.48/1.30	1.50/1.31
Intensity, max/min, units	33.6/21.5	32.9/22.9	33.5/21.9	35.0/22.0

NADC-88141-60 (Volume I)

corresponding to $\psi = 0$. For other values of ψ , this time is adjusted somewhat, specifically lengthened, to account for increased absorption for nonzero ψ , so that consistent measurements are made at all ψ . The setting of the actual counting time is done automatically by the control software of the TEC system.

Studying the various test parameters and the resulting x-ray stresses and error bands leads to several general conclusions: 1) The x-ray stresses (prior to yielding) in virtually all cases agree with the applied stress within the error band. 2) A counting time for each diffraction peak of 75 sec. is too short, 100 sec. seems adequate, but 150 sec. is even better. 3) The use of 10 different ψ angles, that is, observation of 10 different diffraction peaks, definitely improves the quality of the measurement compared to 6 values of ψ . 4) Oscillation of ψ is beneficial.

Use of 150 sec. and 10 values of ψ results in a total time of about 30 minutes to obtain one x-ray stress value. A combination of 100 sec and 10 values, resulting in 20 minutes total, represents a reasonable compromise where time is limited. Note that counting times are long for titanium alloys compared to other structural metals due to the low rate of photon production and the high fluorescent background, which results in the need for more data to resolve the resulting signal-to-noise ratio problem. Total measurement times of 5 or perhaps 10 minutes would generally be sufficient for aluminum alloys, steels, etc.

Cyclic Loading

X-ray stress data were taken at various levels during the first four cycles of zero-to-maximum loading of a notched, electropolished specimen. These data are plotted versus the applied net section nominal

NADC-88141-60 (Volume I)

stress in Fig. 16. A downward drift during load cycling of the stresses in Fig. 16 would indicate relaxation of the mean stress. If any occurred in this particular case, it is small and difficult to distinguish from the scatter in the data.

In Fig. 17, the data from Fig. 16 for the first load cycle are compared with the expected local notch stress behavior as estimated from Neuber's rule, and also elastic unloading following the yielding which occurs on loading. The same type of anomalous decrease in x-ray stress following yielding that was previously observed is seen in Fig. 16. As expected, the unloading is approximately linear and parallel to a line of slope equal to k_t , the elastic stress concentration factor for the notch. However, the anomalous drop in x-ray stress that occurred during yielding is retained during this elastic unloading. The residual stress at zero load is measured by x-rays to be 78 ksi, which differs considerably from the estimated value of 37 ksi. The lattice spacing plot giving this 78 ksi residual stress, shown in Fig. 18, does not appear to be unusual in any way.

Discussion of the Unexplained Behavior After Yielding

The reason for the anomalous decrease in x-ray stress beyond yielding is not known. Some possibilities are: 1) measurement error of some type, 2) altered x-ray elastic constants due to some second order effect of the plasticity, 3) actual lower stresses in a thin surface layer than in the bulk of the specimen due to some unexplained aspect of the material behavior, and 4) effects of multiple structural phases in the material.

The first possibility (error) seems unlikely, however, as good agreement is obtained up to the beginning of yielding. It is also

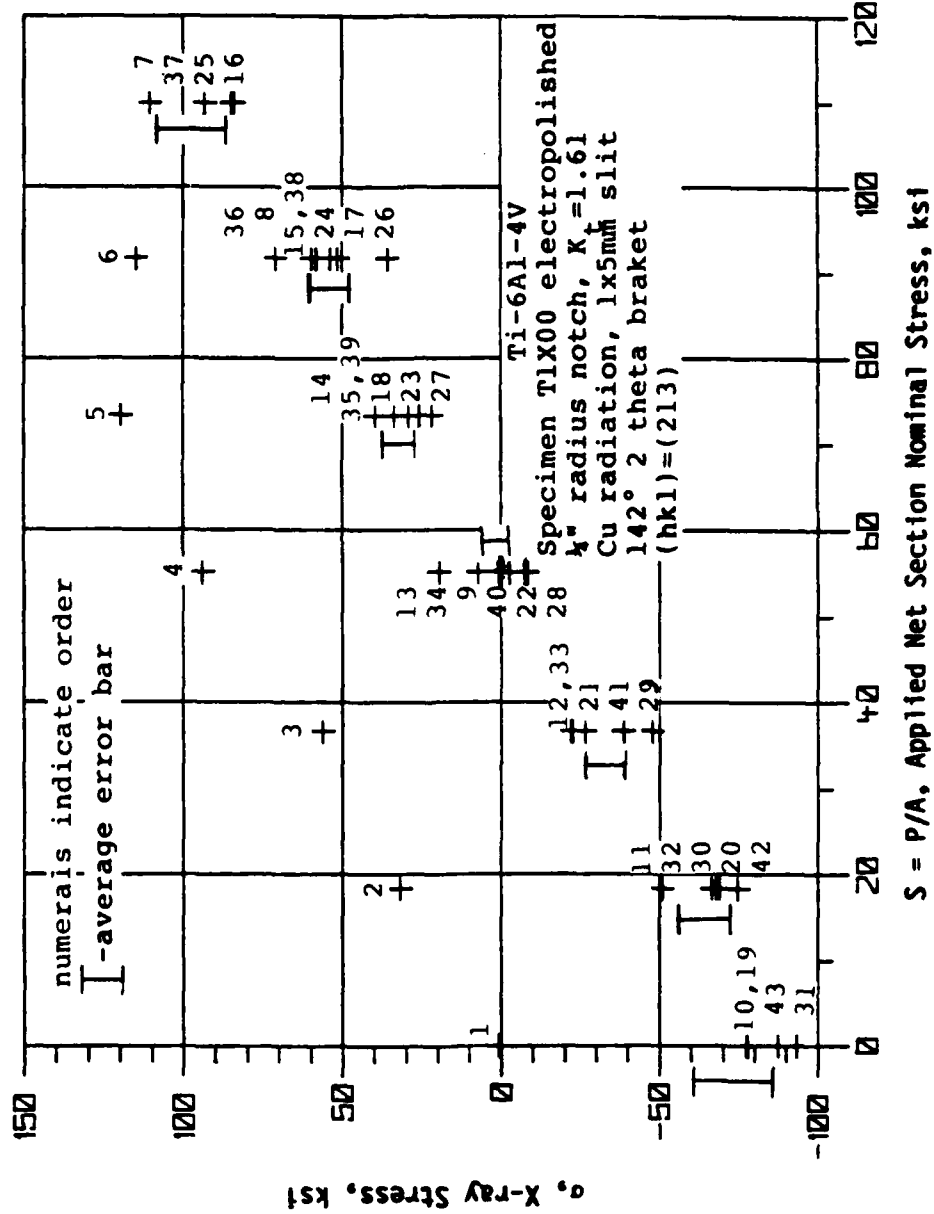


Fig. 16 - Stresses measured by x-ray diffraction during four cycles of zero-to-maximum loading of a notched electropolished titanium specimen. The maximum load is 12.0 kips (P/A = 110.0 ksi.)

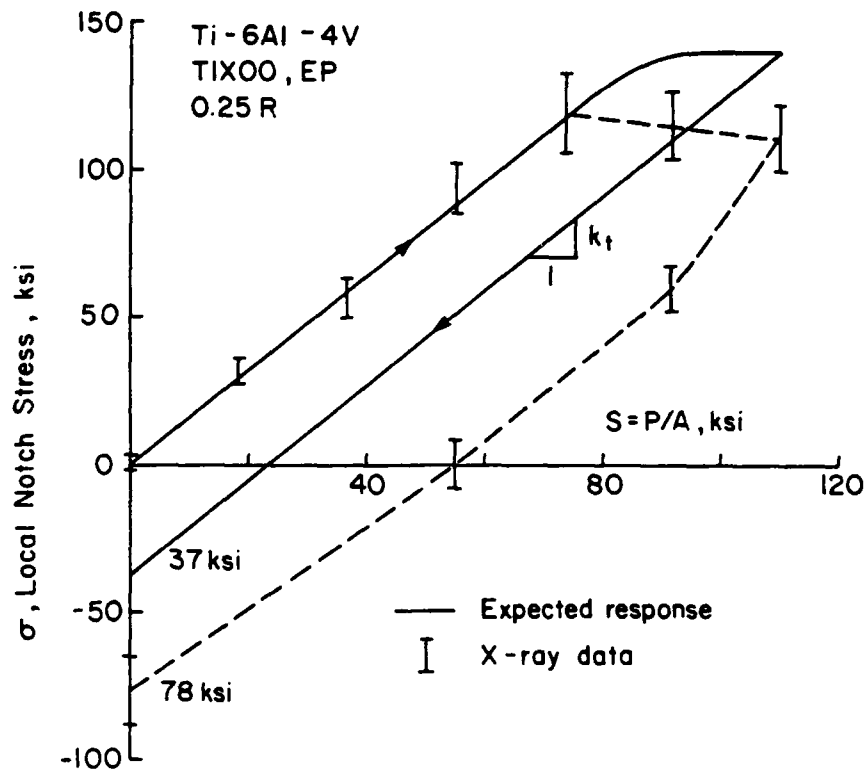


Fig. 17 - Comparison of estimated local notch stress response with x-ray data error bars for the first cycle of zero-to-maximum loading of the notched specimen.

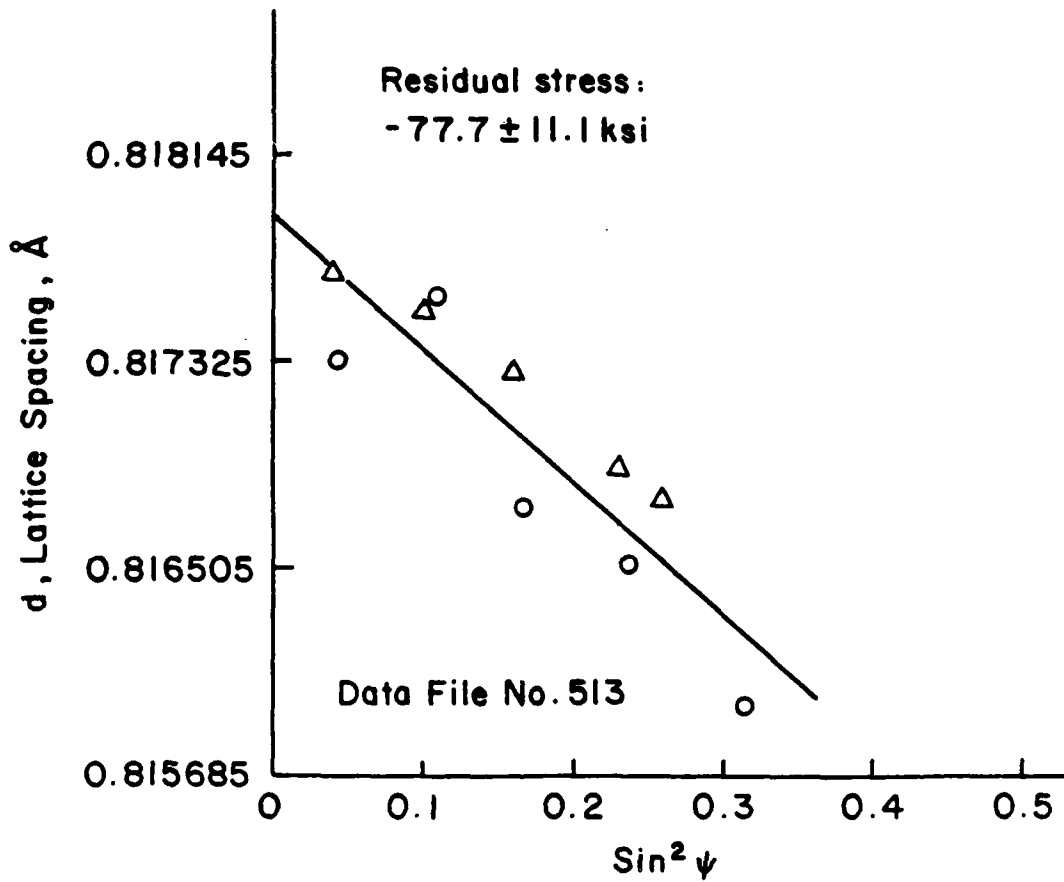


Fig. 18 - Data and fitted line for x-ray measurement of residual stress at zero load after the first cycle of zero-to-maximum loading.

NADC-88141-60 (Volume I)

difficult to explain changes in the elastic constants for Eq. 2 which are sufficient to cause the rather large discrepancy. Since we are fairly certain that the lattice spacings are accurately measured, it appears to be difficult to escape the conclusion that the stress in a thin surface layer does actually decrease. Such behavior is not readily explained by the concepts of plasticity and structure of materials in current use. Its confirmation by further study could have considerable significance.

NADC-88141-60 (Volume I)

EVALUATION OF THE X-RAY SYSTEM

The system used is specifically a Prototype Model 1610-2 Portable X-ray Diffraction Residual Stress Analyzer, made by Technology for Energy Corp., Knoxville, TN, for the U.S. Navy under Contract No. N00019-85-C-0419. It was delivered to Virginia Polytechnic in April of 1987 and is on loan to VPI by the U.S. Navy for the duration of this project.

The University and State of Virginia radiation safety requirements were finally met in July of 1987. (The delay was primarily due to the necessity of fabricating hardware to meet the extra closed-beam operation requirements imposed by the University because of planned student use of the system). In the seven months since then, the unit has been used extensively, with the total operation time to date being approximately 800 hours. Most of this operation was trouble free.

More detailed discussion is given below under subheadings dealing with general utility, accuracy, and maintenance.

General Utility of the Equipment

The performance of the equipment, and especially the automation, make it very efficient to use with a minimum of operator involvement. Special provisions for rigid mounting, and positioning and alignment, of the sample may be needed in the possible future use of such equipment with items of real hardware. Special alignment fixtures analogous to the alignment plate of Fig. 5 could be designed to "lock on" to any real part where complex geometry complicates positioning and where frequent measurements are expected. The current capability is sufficient for flat and gently curving surfaces. Limitations on access similar to the angles α and β of Fig. 2 are an important consideration for future

NADC-88141-60 (Volume I)

practical application of the equipment. Only minor additional improvement in this area is physically possible due to the necessity of making measurements over a range of tilt angles, ψ .

When the safety system stops the machine, there are cases where some additional information would be useful. For example, when there is a low count rate on the computer, the system is shut off as this may indicate that x-rays are not being interrupted by a sample and thus may impinge an area where they are hazardous. In addition to no sample being in place, a low count rate could be caused by lack of emission from the x-ray tube, the wrong filter on the detector, or an incorrect detector voltage setting. More specific diagnosis of the problem, or at least a checklist appearing on the computer terminal, would be useful in such cases.

It would be useful to be able to easily turn off the $K_{\alpha 1} - K_{\alpha 2}$ correction that is automatically done by the computer for all measurements. At present, the procedure for doing this is not obvious and is not explained in the manual. This ability is sometimes needed to ascertain the magnitude of the correction being made, and to permit measurements without it where desired.

Some improvements could be made in the explanation of the stress report produced by the computer. A concise description and/or summary should be provided in one place, where it can be quickly located, of the values printed in the x-ray stress report. Topics could include brief discussions of how values are calculated and x-ray system computer files that are input to the calculations. Also, a brief explanation of what each quantity physically means, along with its physical units, would be useful. Values of specific interest are tilt angle (ψ), intensity,

NADC-88141-60 (Volume I)

FWHM, K_{α} correction, diffraction angle (2θ), lattice spacing (d), standard deviation, counting statistics error, goodness of fit error, and total stress error. The total stress error is calculated as the geometric mean of the other two, but it may be appropriate simply to take the larger of the two as the total error.

Repeatability, Accuracy, and Precision

The repeatability, accuracy, and precision of measurements with the system is judged to be excellent when circumstances are favorable. Data bearing on this matter have already been presented in Figs. 6-11, 13 and 17, and also in Table 2. The anomalous behavior after yielding in Figs. 13 and 17, which was also discussed above, is not thought to be a repeatability, accuracy, or precision problem, but a more fundamental area that needs research.

Where circumstances are not favorable, such as for large crystallographic grain size, preferred orientation, or unusual states of stress, inaccuracies can be a problem. It is especially important that operators of this equipment be trained to recognize such problems so that engineering decisions are not made based on invalid data. Specific guidelines for assuring that such problems do not exist are needed. Additional software development should be considered so that such guidelines are automatically presented to the operator. Changes in setup parameters or additional data analysis could then be used to obtain valid data in some cases, and the remaining cases identified where the data should not be used for engineering purposes. We understand that TEC is pursuing additional software development that at least partially addresses this need. Although many of these considerations are covered in the standard training given by TEC to purchasers of the

NADC-88141-60 (Volume I)

equipment, such additional software would have the advantage of minimizing the chance of difficulties with untrained operators or those whose training is not current.

Maintenance

Some equipment breakdowns did occur during the extensive usage of the equipment, but not more than is typical of sophisticated laboratory equipment in general. For example, there was a failure in a circuit board of the computer and one in the air conditioner cooling unit, both of which were readily repaired. However, for the computer failure, more than two weeks were lost in diagnosing the problem. The total downtime in the seven months of usage has been approximately 6 weeks. About two-thirds of this time was associated with simply diagnosing problems. Note that the modular design of the equipment facilitates repair. But the complicated interactions among 22 subsystems, as influenced by the computer controlled environment, sometimes makes isolation of a problem very difficult.

Maintenance was complicated by the fact that no product warranty or service contract was in place. This situation was simply a result of the terms of the contract between the Navy and TEC under which the equipment was developed. Nevertheless, TEC personnel have been very cooperative and helpful to us in dealing with maintenance problems.

TEC has suggested a \$25,000 a year service contract, which would include labor, materials, repairs on a 48-hour turnaround basis, and all software upgrades. This amount seems reasonable, being about 12% of the value of the equipment, which is in the range seen for other complex lab equipment. Although funds are not available for this on the current

NADC-88141-60 (Volume I)

project, such an arrangement seems advisable in general for serious users of the equipment.

For use under shop or field conditions, special care will thus be needed to assure that the expertise and parts necessary for service are readily available. Comments about some specific problem areas where the system could be improved are given below.

Maintenance problems occurred twice which were caused by the high voltage connection which supplies power to the x-ray tube. In particular, an arc to ground can occur when the power is turned on. When this occurs, the power to the x-ray high voltage power supply, the computer, and all the other electronics is sometimes briefly interrupted. The computer will then sometimes reboot along with the x-ray diffractometer servomotor running away to some unknown value of ψ tilt. This is a problem in that the diffractometer may strike obstructions in its path, especially if measurements are being made in areas of reduced clearance. Turning off the computer does not stop the runaway motion, only turning off the power to the computer A/D and safety systems, or shutting off the power completely to the chasis, is effective.

This problem with the power cable has been temporarily solved by replacing parts and maintaining a high degree of cleanliness. A more permanent solution involving some local redesign may be possible. It is noteworthy that the more recent units sold by TEC have an on/off switch for the shaft encoder motor drive, which would allow the operator to quickly stop the motion. The circuitry that controls the shaft encoder motor drive has also been redesigned in recent units and is now less sensitive to this problem.

NADC-88141-60 (Volume I)

The articulated arm from which the diffractometer can be mounted can exert considerable moment on the slide that is elevated by a motorized power screw in the tower of the chasis. This moment is transferred to the slide from the arm by friction between the slide's surface and the mating surface of the arm with pressure supplied by bolts. This arrangement is unreliable in that the mating surfaces shift. The moment must then be carried directly by the bolts, which are now loaded in shear along with the tensile forces they carry. Also, when the shift occurs, rubbing takes place along the sides of the channel in the tower provided for the slide and the arm.

Stops, pins, and/or bearing surfaces to prevent this twisting would provide a temporary solution. Redesign of the bolted joint so that bolt preloads provide sufficient friction to prevent any slippage would be the straightforward and permanent solution. This problem appears to occur only in the new lightweight tower designed for this special prototype unit. TEC informs us that similar problems do not occur in their standard tower design.

NADC-88141-60 (Volume I)

DISCUSSION AND PLANS

The capability for making x-ray stress measurements in test specimens during brief pauses in fatigue tests has been developed essentially as far as current technology allows. Two problems remain. One is that preferred orientation (texture) in the particular batch of aluminum alloy being used makes work with this material difficult. The other is that poorly understood behavior occurs upon yielding. The assessment of both of these problems is that their solution will require advanced work in x-ray diffraction theory and materials science that is beyond the scope of this project. Therefore, only limited further study of these complexities will be done in this project.

In the remainder of the project, the stress-strain modeling effort will be emphasized and concluded. This effort will be supported by x-ray diffraction work to the extent that is feasible. In particular, due to the difficulty with aluminum, titanium will be emphasized as far as confirmation of the model by measurement of x-ray stresses is concerned. Equivalent modeling work will be done on aluminum, but not confirmed by x-ray unless a method of obtaining valid data in the presence of the texture can be found without extensive research.

Unless an explanation can be found without extensive research, the anomalous behavior upon yielding will be handled by attempting to develop corrections for it. This will be done in an empirical manner based on data for unnotched specimens where the applied stress is known.

NADC-88141-60 (Volume I)

CONCLUSIONS

Local stresses can be measured by x-ray diffraction in notched test specimens during brief pauses in fatigue tests. Measurements in 7475-T651 Al are complicated by a texture in the particular batch this material used, with better results being obtained for Ti-6Al-4V. However, anomalous behavior occurs upon yielding which needs to be understood, or at least corrected for.

The x-ray system performed very well under extensive usage. The automated control and data reduction features of this system are especially valuable. Some, but not excessive, maintenance problems occurred. Rapid diagnosis of maintenance problems in this complex system is especially important in minimizing downtime. Additional guidelines would be useful to aid in data interpretation where complications such as texture, large grain size, or unusual states of stress occur.

NADC-88141-60 (Volume I)

REFERENCES

1. "TEC Model 1600 X-Ray Stress Analysis System Operation and Maintenance Manual," Technology for Energy Corp., Knoxville, TN, 1985.
2. James, M. R., and Cohen, J. B., "The Measurement of Residual Stresses by X-ray Diffraction Techniques," Treatise On Materials Science and Technology, Vol. 19, ed. by H. Herman, Academic Press, New York, 1980.
3. Hendricks, R. W., Virginia Polytechnic Institute and State University, Blacksburg, VA, paper to be published.
4. James, M. R., "Improvements in Residual Stress Determination Through the Use of ψ -Angle Oscillation," Application Note AP-100-04, Technology for Energy Corp., Knoxville, TN, August 1986. (Dr. M. R. James is employed at Rockwell Science Center, Thousand Oaks, CA.)

NADC-88141-60 (Volume I)

APPENDIX A

**X-RAY RESIDUAL STRESS MEASUREMENTS
IN NOTCHED TEST SPECIMENS**

N.E. Dowling

R.W. Hendricks

K. Ranganathan

NADC-88141-60 (Volume I)

INTRODUCTION

Knowledge of the changing state of residual stress at various locations in a fatigue specimen, especially at the root of the notch, is of critical importance in advancing our understanding of the theory and mechanism of fatigue failures [Refs. A-1 to A-3]. The theory of residual stress measurements using x-ray diffraction has long been known and is the subject of several reviews and conferences. (For example, see Refs. A-4 to A-7) This technique, however, has not been compatible for use on a test specimen mounted in a mechanical testing machine due to the geometry of the equipment and the excessive time requirements to make the measurements. These difficulties can be overcome by using a compact and portable x-ray stress analysis system equipped with a position-sensitive proportional counter (PSPC) and an on-line computer system for automated data acquisition and reduction.

It is the purpose of this paper to report residual stress measurements for notched fatigue test specimens of 7475-T651 aluminum and mill-annealed Ti-6Al-4V in a configuration which simulates work to be performed in a mechanical testing machine. The objective of the research is to demonstrate the feasibility of measurements in this situation and to understand the various sources of error encountered and how they can be minimized. Errors discussed in the following sections include counting statistics, grain size and preferred orientation in the specimen, and the effect of notch geometry on x-ray optics errors.

X-RAY DIFFRACTION

For a specimen in a state of biaxial stress, it can be shown (Refs. A-4, A-5) that the lattice spacing, d_h , of atomic planes whose normal

NADC-88141-60 (Volume I)

make an angle ψ with the respect to the normal to the surface is given by

$$\frac{d_{\phi,\psi} - d_{\phi,0}}{d_{\phi,0}} = \left(\frac{1+\nu}{E}\right) \sigma_{\phi} \sin^2 \psi \quad (\text{A-1})$$

In Eq. (A-1) the subscript ϕ refers to the angle the plane of the diffractometer makes with a convenient coordinate system associated with the sample and defines the direction in the sample surface in which the measurements are made, and E and ν are Young's modulus and Poisson's ratio, respectively, for the chosen crystallographic planes. In practice, diffraction peaks are obtained for several values of ψ , and the stress is determined from the slope of data points on a plot of d_{ψ} versus $\sin^2 \psi$. If the stresses are not biaxial, and if there is a shear stress component in the plane perpendicular to the sample, then there is an additional term in Eq. (A-1) which depends on $\sin(2\psi)$. This causes an easily observed splitting in the d_{ψ} versus $\sin^2 \psi$ graph.

The measurements were made with a Technology for Energy Corporation Model 1600 X-ray Stress Analysis system. The diffractometer consists of an arc-shaped track on which moves the carrier plate holding the x-ray tube, collimator, shutter, position-sensitive proportional counter, mounting brackets, and shaft encoder and motor drive assemblies. Alignment of the sample with respect to the center of rotation of the diffractometer is obtained with a mounting plate attached to the track. The position-sensitive proportional counter (PSPC) has the capability of recording not only the presence of a photon, but also its location along a line, with the result that an entire Bragg peak can be recorded simultaneously from a range of 2θ angles without moving the

NADC-88141-60 (Volume I)

diffractometer. Hence, the only diffractometer motion needed is that for changing ψ to obtain diffraction peaks at several values of ψ . A further advantage of the PSPC, indeed the key performance parameter which makes portable x-ray diffractometry even possible, is the fact that its signal-to-noise ratio is greatly improved compared to the detectors used in classical diffractometers. Specifically this ratio is better by a factor between 200 and 1000, allowing the use of small, low power x-ray tubes.

The system employs automated data acquisition and direct reduction of this data using a digital computer, so that handling of data and human involvement with the data is minimal. All standard diffraction corrections, such as determining the maximum of the diffraction peak, background, absorption, Lorentz polarization, and $K\alpha_1 - K\alpha_2$ corrections, are performed on-line. Combined with automated positioning, this results in a total measurement time on the order of a few minutes. This can be a critical factor as in studying time-dependent relaxation of residual stress, as the phenomenon can be studied in detail on a time scale of a few hours.

A distinct advantage of such a system is that it is highly compact, portable, and can be operated in any orientation. The instrumentation can be mounted for work on a specimen in a mechanical testing machine and can remain in position for measurements during brief pauses in a fatigue test. This avoids lost data due to the delay that would otherwise be involved in removing the test specimen for study. It also lessens the chance of accidental damage or compromised specimen alignment, both of which are more likely if test specimens must be repeatedly removed and remounted in the testing machine.

NADC-88141-60 (Volume I)

SPECIMENS AND ALIGNMENT

The alloys of interest in our research are 7475-T651 aluminum and mill-annealed Ti-6Al-4V. Metallography indicates grain sizes in the range 10 to 15 μm in both materials. A semiquantitative analysis of the integrated x-ray intensity as a function of sample orientation is consistent with an approximate (110) $[\bar{1}\bar{1}2]$ rolling texture in the aluminum alloy [Ref. A-8]. There was no indication of texture in the titanium alloy.

Three sample geometries, a straight test section and notches with two different root radii, were used as shown in Fig. A-1. An assembly drawing of the specimen in the fixture impinged by x-rays is shown in Fig. A-2. An alignment plate (Fig. A-3) maintains positioning of the test specimen relative to the x-ray system in the three orthogonal directions. This plate is rigidly attached to the x-ray system and is prealigned and positioned to assure that the surface of the sample is precisely on the center of rotation of the diffractometer, that the normal to the surface is parallel to the diffraction vector at $\psi = 0^\circ$, and that the irradiated volume of the sample remains the same for measurements at all ψ angles.

Shoulders on the specimen above and below the notched region, as at A in Fig. A-2 are closely centered and located, by tolerances of ± 0.0005 in., with the top and bottom of the alignment plate to assure correct positioning in the vertical direction (y on Fig. A-2). The specimen also fits into a slot in the alignment plate. The bottom of this slot fits against the edge of the specimen above and below the notch region, as at B in Fig. A-2, to give positioning in the width direction (x on Fig. A-2). Finally, positioning in the thickness

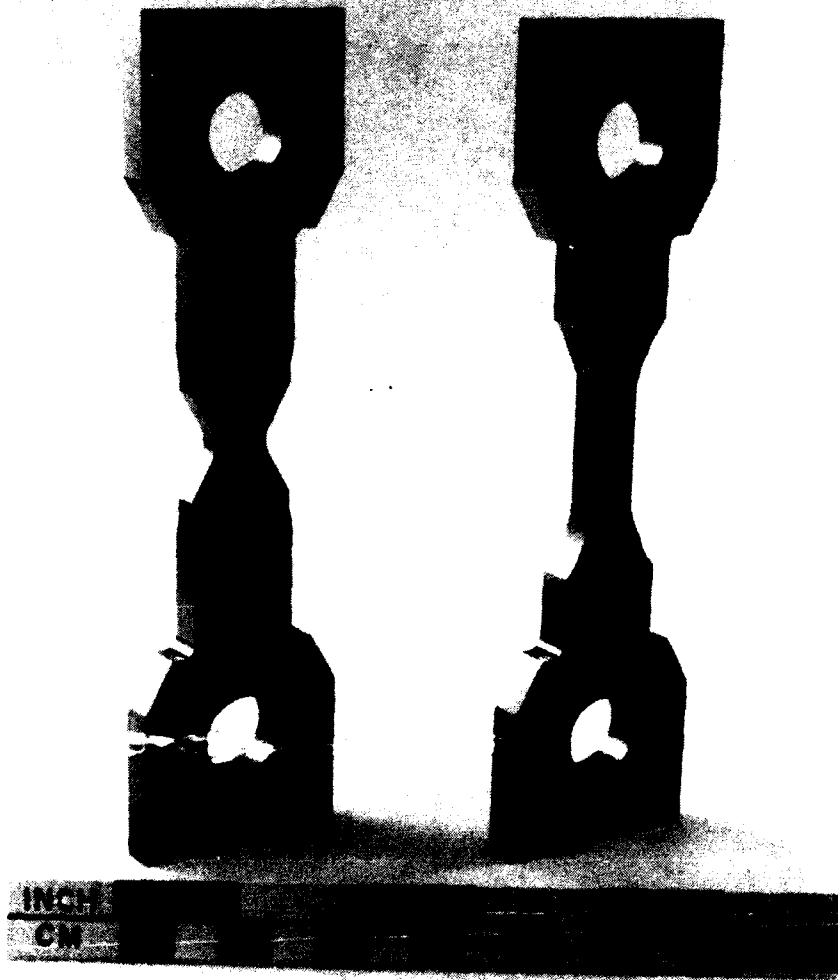


Fig. A-1 Notched and straight test specimens. (The second notch geometry is the same as the one shown except that the notch radius is half as large.)

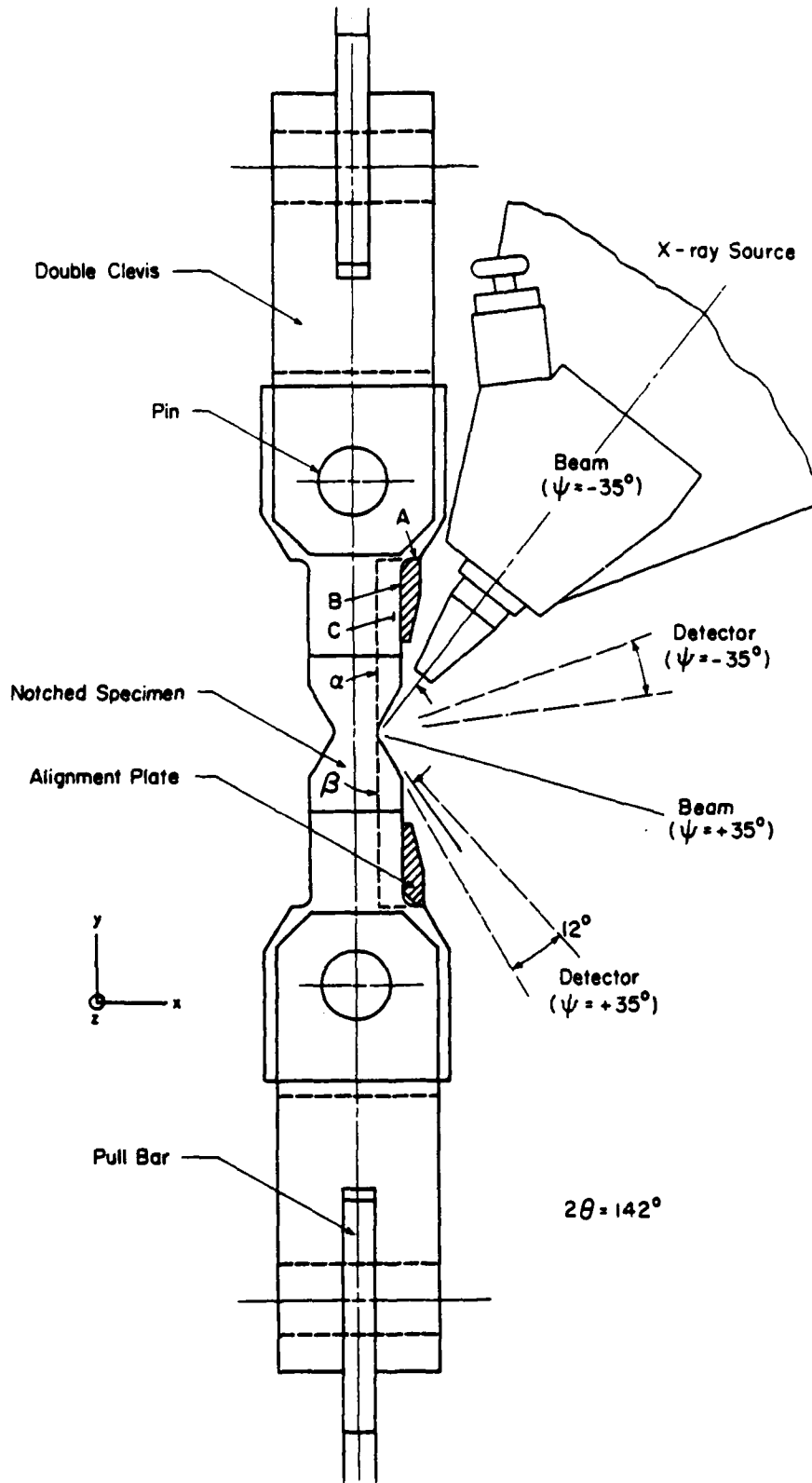


Fig. A-2 Arrangement of specimen, fixtures, and x-ray source, for measurements during mechanical testing.

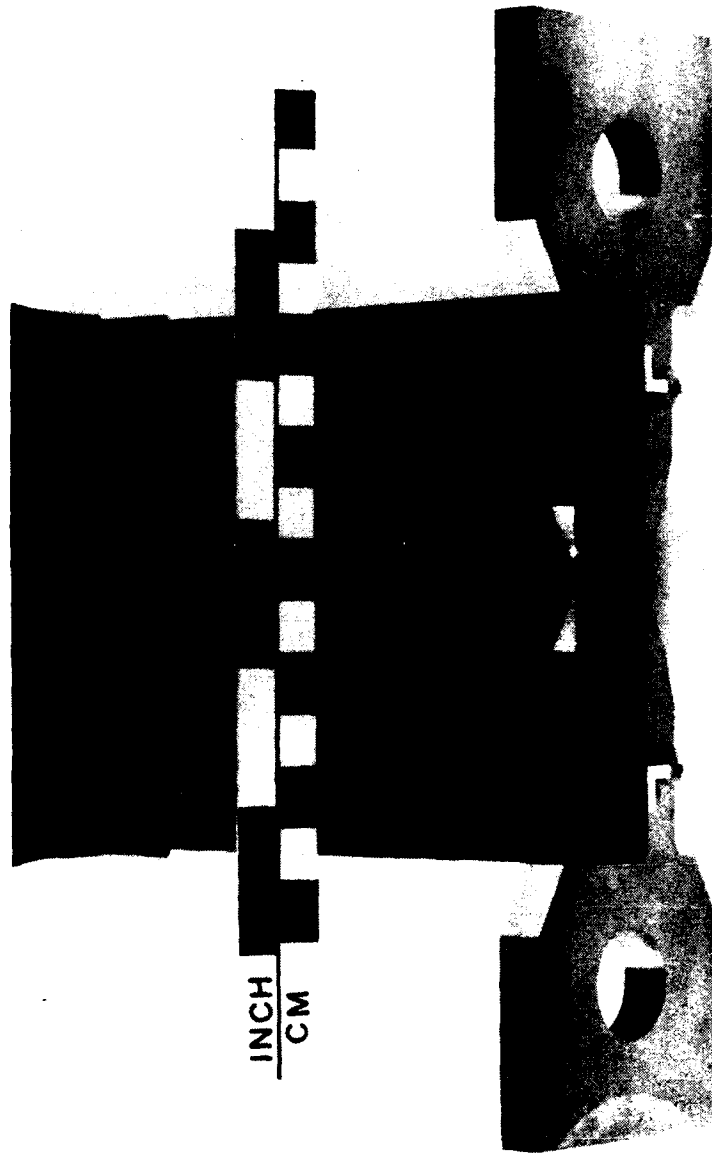


Fig. A-3 Test specimen mounted on alignment fixture.

NADC-88141-60 (Volume I)

direction (z on Fig. A-2) is achieved by fitting the sides of this slot closely to the sides of the specimen above and below the notch region, as at C in Fig. A-2.

The design of the notch is of critical importance. Deep, small-radii notches are required if the stress state is to be reliably estimated from published theory. However, to measure the stresses at the root of the notch by x-ray diffraction, it is required that the flank angle not exceed 30° from the longitudinal center line of the specimen as shown in Fig. 4. With notch radii of 3.175 mm and 6.35 mm, the stress concentration factors are 2.02 and 1.61, respectively [Ref. A-9]. These values include the effect of removal of the material to this flank angle, which effect is about 5% for the sharper notch and less for the blunter notch [Ref. A-10].

NOTCH GEOMETRY

A detailed consideration of the experimental configuration shown in Figure A-2 suggests several potential pitfalls which must be overcome. Stress gradients around the notch required that the x-ray beam be small compared to the notch radius. However, short measuring times require that the maximum possible x-ray power be incident on the sample and thus imply large beam sizes. This problem is mitigated to some extent through the use of rectangular slits, 5 mm long and of varying widths. The long dimension was placed parallel to the specimen thickness, that is, the z-axis in Fig. A-2.

Computations have shown that it is necessary that the notch radius be about 6 or more times larger than the x-ray beam width in order to minimize errors introduced by stress gradients in the root of the notch

NADC-88141-60 (Volume I)

[Ref. A-10]. Additional complications result from deviations of the sample surface from the diffractometer focusing circle, which is dependent on both the Bragg angle, θ , and the tilt angle, ψ [Ref. A-11]. For a beam width of 1 mm, the notch radius r , should not be smaller than about 6 mm as is illustrated in Figure A-4. In particular, when the incident beam is parallel to the flank of the notch, a beam of thickness $r/6$ covers a distance of $r/3$ in the bottom of the notch as shown in Fig. A-4. Any larger beam size would result in diffraction from areas where the stress is significantly below the maximum value in the notch, and thus errors due to stress gradient would be encountered. Based on this notch geometry, computations have shown that the focusing circle errors due to the curvature of the notch will be less than 15 MPa for both materials [Ref. A-10].

For maximum accuracy in stress determinations, it is desirable to cover as wide a range of $\sin^2\psi$ as possible. Further, in order to determine if shear stresses are present, it is necessary to make measurements for both positive and negative ψ angles. The maximum range of ψ -angle allowed by the diffractometer is -45° to $+60^\circ$ for $2\theta = 156^\circ$. These maximum ranges can be achieved for measurements on flat surfaces but are reduced significantly for the test specimens, more so at positive ψ for the notched ones than the straight ones. Also, the diffractometer needs to be attached to the loading frame posts of an electrohydraulic materials testing system. Thus, the grips and the specimen ends may impose additional limitations on the range of possible ψ angles. By careful design of grips and specimen, additional limitations of this type were minimized.

The result achieved is that for notched specimens both the

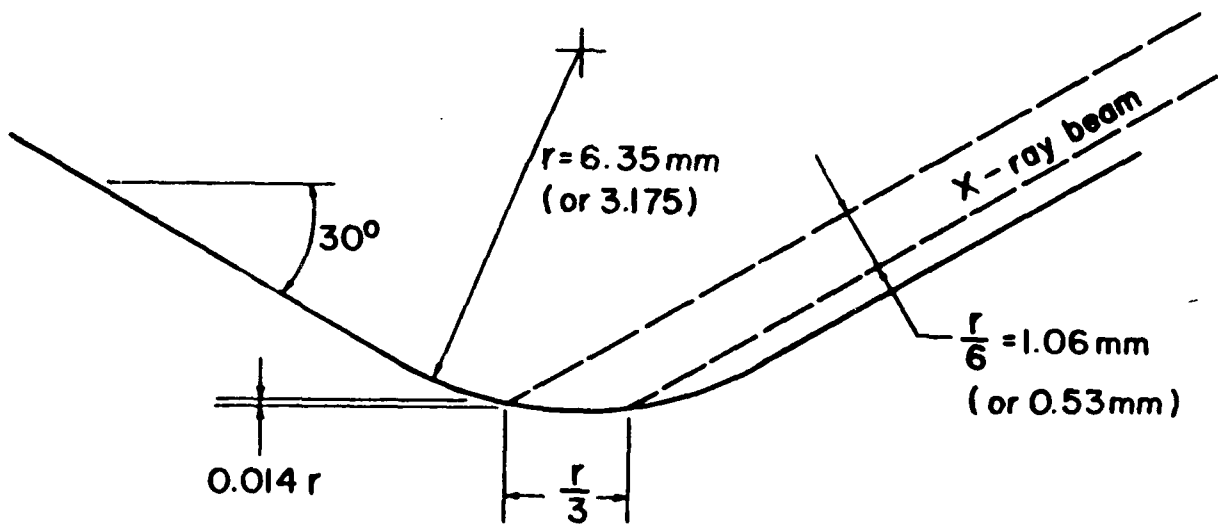


Fig. A-4 Notch geometry.

NADC-88141-60 (Volume I)

angles α and β in Fig. A-2 cannot be smaller than about 36° . The two limits on ψ can be obtained from

$$\psi_{\max} = \theta - \beta \quad (\text{A-2})$$

$$\psi_{\min} = \alpha - \theta$$

so that for notched specimens the limits on ψ are $\pm 35^\circ$ for $2\theta = 142^\circ$, and $\pm 44^\circ$ for $2\theta = 160^\circ$, which are the 2θ angles to be used for the titanium and aluminum alloys, respectively. Also, note that the specimen and grips employed are limited to tensile applied loads. To accommodate compression would require more massive grips closer to the notch, and thus severe and probably unacceptable limits on the feasible ranges of ψ .

Finally, cardboard mock-ups of the grips and fixtures were attached to the specimens to impose the same geometric limitations on the motion of the x-ray system components as would actually occur. It was thus possible to limit data acquisition to ψ -angle ranges which will be encountered in the fatigue experiments and thereby simulate the anticipated experimental errors.

X-RAY MEASUREMENTS

Measurements were made using $\text{Cu } K_\alpha$ diffracted from the $\{213\}$ planes of the titanium alloy at 2θ approximately 142° , and from the $\{333/511\}$ planes of the aluminum alloy at 2θ approximately 160° . A 1.0 mm wide beam was used for titanium, thus requiring a 6.35 mm notch radius, while a 0.5 mm beam could be used for aluminum with a 3.175 mm notch. The experimental parameters are summarized in Table A-1. Typical results are shown in Figs. A-5 and A-6. In addition to the data for d versus $\sin^2\psi$, and the associated errors, the instrument also calculates the

NADC-88141-60 (Volume I)

Table A-1 - Equipment Parameters

Item	Material	
	Ti-6Al-4V	7475-T651 A1
Radiation	Cu	Cu
λ , Angstrom	1.54178	1.54178
2θ , degrees	142	160
Voltage	45000	45000
Amperage	1.85	1.85
Rectangular* Slit Size, mm	1 by 5	0.5 by 5
Measurement Time (per stress value), minutes	20	5

* 5mm dimension parallel to specimen thickness.

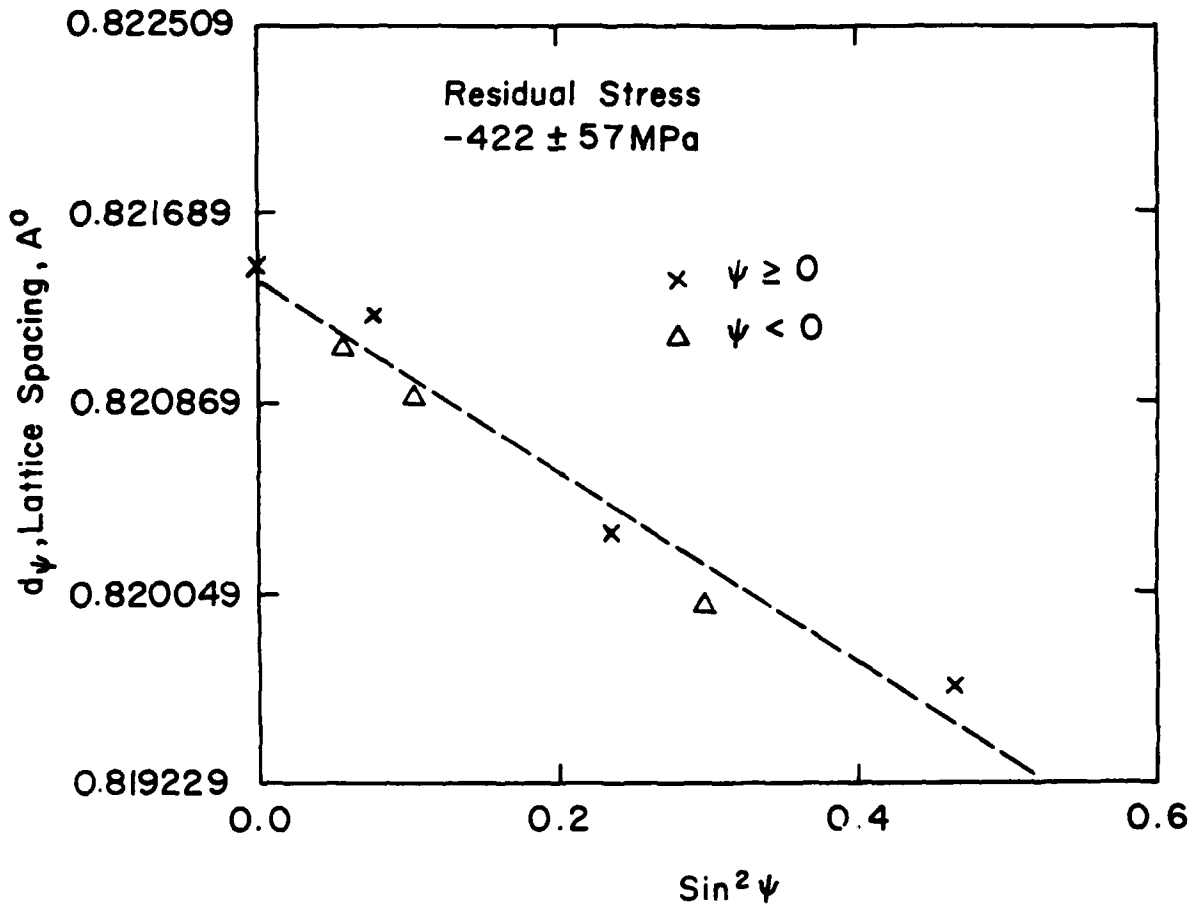


Fig. A-5 Lattice spacing vs. $\sin^2 \psi$ for straight titanium specimen no. T1S02 with a machined surface.

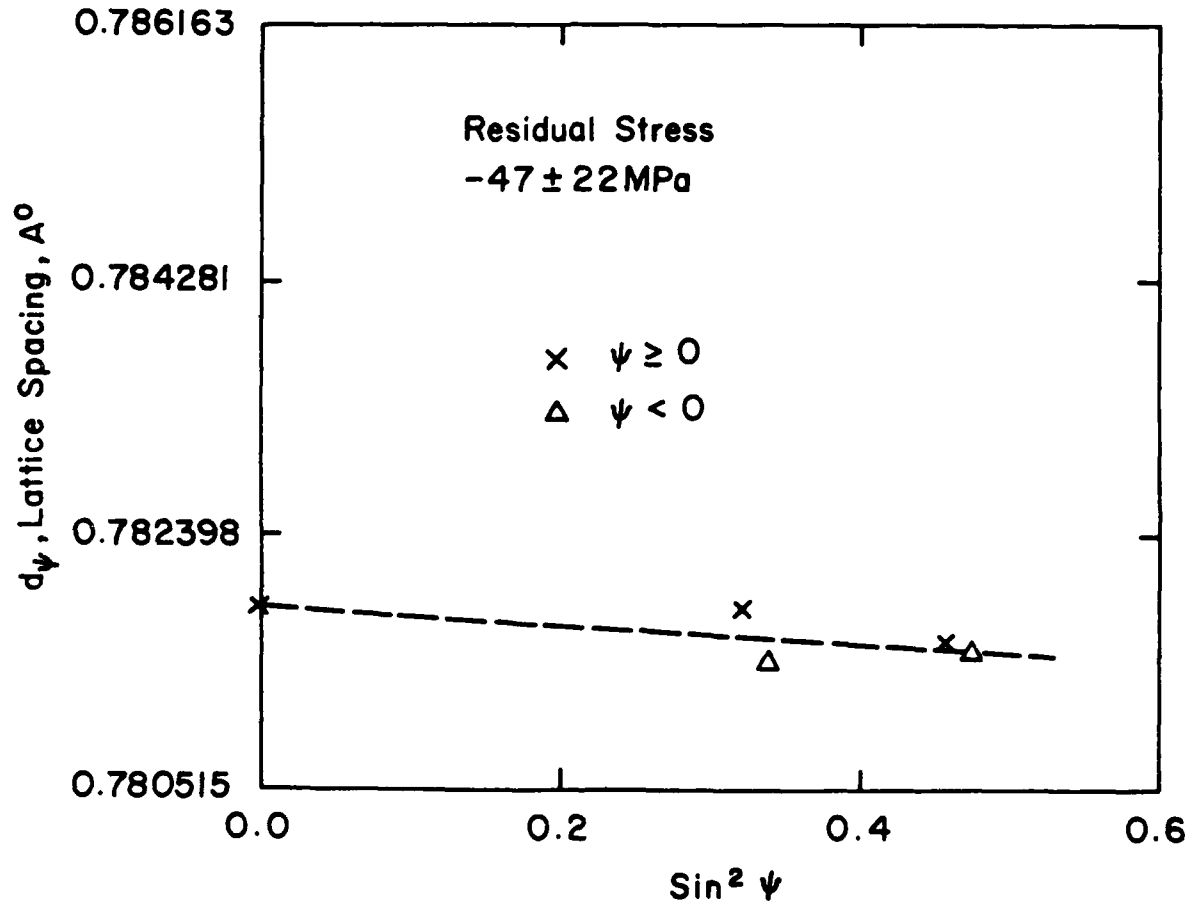


Fig. A-6 Lattice spacing vs. $\sin^2 \psi$ for notched aluminum specimen no. AX23 with an electropolished surface.

NADC-88141-60 (Volume I)

integrated intensity and the full-width-half-maximum (FWHM) of the corrected diffraction peaks. These are useful parameters for monitoring both grains size and preferred orientation effects in the samples.

RESULTS AND DISCUSSION

Table A-2 summarizes measured residual stresses for the two materials and the errors involved for various geometries with either machined or electro-polished surfaces. Also listed are the ψ -angle extremes and the nominal counting time for each measurement.

The errors in the measured residual stress as given in Table A-2 are of two kinds. The counting statistics error is dependent on the counting time. Increasing the counting time by a factor of 2 reduces this error by $\sqrt{2}$. The other type of error is the goodness of fit error, which describes how well a straight line fits the data for the lattice spacing, d_{ψ} , versus $\sin^2\psi$ plot. If the goodness of fit error is significantly larger than the counting statistics error, this implies that the simple assumption of biaxial stress in an isotropic, homogenous material is no longer valid. This could result from grain-size, preferred-orientation, or triaxial stress effects. The goodness-of-fit error includes the counting statics error and thus, in principle, should be larger. However, if only a small number of ψ -angle data points are measured it is possible that the goodness-of-fit error can be less than that from counting statistics. Inspection of the errors in Table A-2 suggests that in most cases the biaxial stress assumption is valid.

Inaccurate stress measurements may be caused by large grain size and/or preferred orientation. Large grain size causes "spotty" Debye-Scherrer patterns and leads to large variations in diffracted

NADC-88141-60 (Volume I)

Table A-2 - Experimental Results

Item	Spec No.			
	T1X10	T1S02	AX23	AX23
Measurement No.	1	2	3	4
Material	Ti	Ti	Al	Al
Notch radius, mm	6.35	none	3.175	3.175
Surface ¹	M	M	E	E
ψ Oscillation Range, degrees	4	4	4	4
ψ Extremes, degrees	±33	-34 +42	±43	±43
Number of ψ Angles Used	5	7	5	5
Counting time at each ψ, seconds	180	180	180	60
Residual Stress, MPa	-315.7	-422.1	-25.9	-46.7
Errors, MPa				
Counting Statis.	81.9	57.4	17.2	16.5
Goodness of Fit	100.0 ²	30.2	183.0 ³	22.4

¹ Machined (M) or electropolished (E).

² Probable alignment error.

³ This large value is caused by texture and appears in only this measurement due to the particular choices of ψ used.

NADC-88141-60 (Volume I)

intensity. Both metallography and independent measurements made at different locations on the flat surface of the specimens indicated that no significant problem in either material resulted from this effect. However, to mitigate any such possible problem, measurements were made with a 4° ψ -angle oscillation. The motor drive on the diffractometer is capable of such ψ angle oscillation and thus improves the precision of the stress values.

A problem due to texture was encountered in aluminum (measurement 3 of Table A-2), with the result that all of the residual stress values in Table A-2 for this material are in question. Texture is generally evidenced by both a nonlinear d_ψ versus $\sin^2\psi$ plot and by variations in the integrated intensity for various (ϕ, ψ) orientations. Further work, by which a crude pole figure was developed by potting the integrated intensity at various (ϕ, ψ) locations on a stereographic projection indicated a typical face-centered-cubic (110) $[\bar{1}\bar{1}2]$ rolling texture [Ref. A-8]. It is concluded that this particular material, which was received from the manufacturer as cold-rolled plate, is not amenable to residual stress measurement by x-ray diffraction. However, it must be noted that more recently we have obtained a block of the same alloy in a forged condition from the Naval Air Rework Facility in Norfolk, VA. X-ray residual stress studies on this material, both at Norfolk [Ref. A-12] and at VPI [Ref. A-13], do not show any signs of significant preferred orientation. Quick and reliable means of detecting the presence of texture are needed so that invalid residual stress data are not used for engineering purposes.

Eight measurements including those described in Table A-2 were made during a four hour period, with about half of this time being occupied

NADC-88141-60 (Volume I)

by activities other than the measurements. Measurement of one residual stress value on titanium required and elapsed time of about 20 minutes, while on aluminum one measurement required only about 5 minutes. Most of the measurement time is occupied by x-ray photon counting at each ψ angle, with the times involved being given in Table A-2. Note that connecting the specimen and the x-ray system is rapid, requiring only one depth gage micrometer measurement to check the precise alignment of the sample. No time is lost in shifting to different ψ angles, as this is rapidly done by the automated system. Statistical data reduction by the digital computer to obtain the residual stress value is essentially instantaneous. This data reduction includes the appropriate d_{ψ} versus $\sin^2\psi$ plot similar to Figs. A-5 and A-6, plus printouts of all other data, including integrated intensity, correction factors, and FWHM.

The measurements obtained for titanium are judged to be of sufficient accuracy, and are otherwise suitable, for the research which is underway on relaxation of residual stress during fatigue loading. However, similar work on aluminum may require the choice of another batch of material. The significance of the results reported is that they demonstrate the capability for quickly and efficiently making accurate measurements during brief pauses in a fatigue test with the specimen left in place. It should be noted, however, that plastic deformation during testing may cause some additional difficulty with the measurements, and care will be needed in this area.

CONCLUSIONS

The present work demonstrates that the equipment, specimens, and

NADC-88141-60 (Volume I)

fixtures described can be used successfully in a mechanical testing machine to make residual stress measurements on a test specimen during brief pauses in a fatigue test. The measurement times are about 5 minutes per stress value for the aluminum alloy and 20 minutes for the titanium alloy.

NADC-88141-60 (Volume I)

REFERENCES

- A-1. Rosenthal, D., "Influence of Residual Stress on Fatigue," Metal Fatigue, G. Sines and J. L. Waisman, eds., McGraw-Hill (1959) pp. 170-196.
- A-2. Rowland, E. S., "Effect of Residual Stress on Fatigue," Fatigue - An Interdisciplinary Approach, J. J. Burke, N. L. Reed, and V. Weiss, eds., Syracuse University Press, Syracuse, NY (1964) pp. 229-244.
- A-3. Stadnick, S. J., and Morrow, J., "Techniques for Smooth Specimen Simulation of the Fatigue Behavior of Notched Members," Testing for Prediction of Material Performance in Structures and Components, ASTM STP 515, American Society for Testing and Materials (1972) pp. 229-252.
- A-4. James, M. R., and Cohen, J. B., "The Measurement of Residual Stresses by X-Ray Diffraction Techniques," Treatise On Materials Science and Technology, 19, H. Herman, ed., New York: Academic Press (1980).
- A-5. Noyan, I. C., and Cohen, J. B., Residual Stress: Measurement by Diffraction and Interpretation, New York: Springer-Verlag (1987).
- A-6. Macherauch, E. and Hauk, V. (eds.) Residual Stresses, Oberursel: DGM Informationgesellschaft-Verlag (1986).
- A-7. Macherauch, E. and Hauk, V. (eds.) Residual Stresses in Science and Technology, Oberursel: DGM Informationgesellschaft-Verlag (1987).
- A-8. Barrett, C. and Massalski, T. B., (eds.) Structure of Metals (3rd Ed.), Oxford: Pergamon Press (1980) p. 556.
- A-9. Peterson, R. E., (eds.) Stress Concentration Factors, New York: John Wiley and Sons (1974) pp. 34-39.
- A-10. Ranganathan, K., (eds.) A Simulation Model for Stress Measurements in Notched Test Specimens by X-Ray Diffraction, MS Thesis, VPI & SU (1988).
- A-11. Hendricks, R. W., to be published.
- A-12. Fizer, K. W., private communication.
- A-13. Newsome, G., Hendricks, R. W., and Swanson, R. E., unpublished research.

Northrop Corporation
Attn: Dr. Ratwani
One Northrop Avenue
Hawthorne, CA 90250

1 copy

Northrop Corporation
Attn: Mr. Alan Liu
One Northrop Avenue
Hawthorne, CA 90250

1 copy

Rockwell International Science Center
Attn: Dr. F. Morris
1049 Camino Dos Rios
Thousand Oaks, CA 91360

1 copy

University of Dayton Research Institute
Attn: Dr. Gallagher
300 College Park Avenue
Dayton, OH 45469

1 copy

LTV Aerospace and Defense Company
Attn: Dr. C. Dumesnil
P.O. Box 225907
Dallas, TX 75265-0003

1 copy

University of Oklahoma
School of Aerospace, Mechanical
and Nuclear Engineering
Attn: Dr. D. M. Egle
Norman, OK 78301

1 copy

LTV Aerospace and Defense Company
Attn: Mr. T. Gray
P.O. Box 225907
Dallas, TX 75265-0003 1 copy

Boeing Commercial Airplane Company
Attn: Mr. Porter
P.O. Box 3707
Seattle, WA 98124 1 copy

Fairchild Industries
Attn: Technical Library
Hagerstown, MD 21740 1 copy

Grumman Aerospace Corporation
Attn: Dr. H. Armen
South Oyster Bay Road
Bethpage, LI, NY 11714 1 copy

Lehigh University
Attn: Dr. Sih
Institute of Fracture & Solid Mechanics
Bethlehem, PA 18015 1 copy

Lehigh University
Attn: Dr. T. J. Delph
Institute of Fracture & Solid Mechanics
Bethlehem, PA 18015 1 copy

McDonnell Douglas Corporation
Attn: Mr. D. Rich
P. O. Box 516
St. Louis, MO 63166 1 copy

Northrop Corporation
Attn: Mr. A. Liu
One Northrop Avenue
Hawthorne, CA 90250 1 copy

Rockwell International Corporation
Attn: Mr. J. Chang
LA Division/International Airport
P.O. Box 92098
Los Angeles, CA 90009 1 copy

Sikorsky Aircraft
Attn: S. Garbo
110 N. Main Street
Stratford, CT 06622 1 copy

University of Illinois
College of Engineering
Attn: Professor D. Socie
Urbana, IL 61801 1 copy

University of Pennsylvania
Department of Mechanical Engineering
Attn: Dr. Burgers
111 Towne Bldg., D3
Philadelphia, PA 19104 1 copy

Rockwell International Corporation
Attn: Mr. F. Kaufman
4300 East Fifth Avenue
Columbus, OH 43216 1 copy

Rohr Corporation
Attn: Dr. F. Riel
Riverside, CA 92503 1 copy

Boeing Helicopter Company
Attn: C. Gunther
P.O. Box 16858
Philadelphia, PA 19142 1 copy

Douglas Aircraft Company
Attn: Mr. Luce (7-21)
3855 Lakewood Blvd.
Long Beach, CA 90846 1 copy

General Dynamics/Convair
Attn: Mr. G. Kruse
P.O. Box 80847
San Diego, CA 92138 1 copy

Grumman Aerospace Corporation
Attn: Dr. B. Leftheris
South Oyster Bay Road
Bethpage, LI, NY 11714 1 copy

Lehigh University
Attn: Prof. R. Wei
Institute of Fracture & Solid Mechanics
Bethlehem, PA 18015 1 copy

Lockheed Aeronautical Systems Co. - Georgia
Attn: Mr. T. Adams
86 S. Cobb Drive
Marietta, GA 30063 1 copy

Lockheed Aeronautical Systems Co. - Georgia
Attn: M. B. M. Shah
86 S. Cobb Drive
Marietta, GA 30063 1 copy

National Aeronautical & Space Adm
George C. Marshall Space Flight Ctr
Attn: Technical Library
Huntsville, AL 35812 1 copy

National Aeronautical & Space Adm
Lewis Research Center
Attn: Technical Library
Cleveland, OH 44135 1 copy

Air Force Systems Command
Attn: AFWAL/FDS
Wright Patterson Air Force Base
OH 45433 1 copy

Air Force Systems Command
Attn: AFWAL/FDSA
Wright Patterson Air Force Base
OH 45433 1 copy

Air Force Systems Command
Attn: AFWAL/FDSE
Wright Patterson Air Force Base
OH 45433 1 copy

ALCOA
ALCOA Labs
Attn: Mr. J. G. Kaufman
ALCOA Center, PA 15069 1 copy

Bell Helicopter Company
Textron Inc.
Attn: T. Haas
P.O. Box 482
Ft. Worth, TX 76101 1 copy

Boeing Helicopter Company
Attn: W. Kesack
P.O. Box 16858
Philadelphia, PA 19142 1 copy

General Dynamics Corporation
Attn: Dr. S. Manning
P.O. Box 748
Ft. Worth, TX 76101 1 copy

Grumman Aerospace Corporation
Attn: H. Eidenoff
South Oyster Bay Road
Bethpage, LI NY 11714 1 copy

Lockheed Aeronautical Systems Company
Attn: Mr. J. Ekvall/76-23, Bldg. 63
P. O. Box 551
Burbank, CA 91520 1 copy

Lockheed Aeronautical Systems Company
Attn: Mr. E. Walker/76-23, Bldg. 63
P.O. Box 551
Burbank, CA 91520 1 copy

McDonnell Aircraft Company
McDonnell Douglas Corporation
Attn: R. Pinckert
P.O. Box 516
St. Louis, MO 63166 1 copy

Federal Aviation Administration
800 Independence Avenue, SW
(Attn: Mr. J. Soderquist)
Washington, D.C. 20591 1 copy

National Aeronautics & Space Adm
Langley Research Center
Attn: Mr. C. E. Harris/MS188E
Hampton, VA 23365 1 copy

Army Materials Technology Laboratory
Attn: D. Oplinger/SLCMT-MS
Watertown, MA 02172-0001 1 copy

National Technical Information Center
U. S. Department of Commerce
Springfield, VA 221512 2 copy

Oklahoma City Air Logistics Center
Attn: MAQCP
Tinker Air Force Base
Oklahoma 73145 1 copy

United States Army
Research Office
Durham, NC 27701 1 copy

Defense Technical Information Center
Attn: Administrator
Building #5, Cameron Station
Alexandria, VA 22314 2 copies

U.S. Army R&D Center
Attn: STRBE-VC/L. Ryan
Fort Belvoir, VA 22060-5606 1 copy

Battelle Columbus Laboratories
Attn: Dr. B. Leis
505 King Avenue
Columbus, OH 43201 1 copy

Drexel University
Attn: Dr. Auerbuch
32nd and Chestnut Streets
Philadelphia, PA 19104 1 copy

Director
Naval Research Laboratory
Attn: Dr. R. Badaliane
Washington, DC 20375 1 copy

Sacramento Air Logistics Center
Attn: MANE/A. J. Hammond
McClellan Air Force Base
Sacramento, CA 95652 1 copy

Metals and Ceramics Information Ctr
Battelle Columbus Laboratories
505 King Avenue
Columbus, OH 43201 1 copy

Warner-Robbins Air Logistics Ctr
Attn: MMSRD/Mr. T. Christian
Robins Air Force Base
Georgia 30198 1 copy

Army Applied Technology Directorate
U.S. Army Aviation Research & Technology Activity
Attn: SAVRT-TY/H. Reddick
Fort Eustis, VA 23604-5577 1 copy

Ogden Air Logistics Center
Attn: MANCC
Hill Air Force Base
Utah 84055 1 copy

San Antonio Air Logistics Center
Attn: MMETM
Kelly Air Force Base
San Antonio, TX 78241 1 copy

NASA Headquarters
Attn: Dr. D. Mulville
OAST-Code RM
Washington, D.C. 20546 1 copy

Commander
Naval Air Engineering Center
Attn: Mr. F. Sinatra
Lakehurst, NJ 08733 1 copy

Commander
Naval Air Engineering Center
Attn: Mr. Neil Goodis
Lakehurst, NJ 08733 1 copy

Commanding Officer
Naval Aviation Depot
Attn: Technical Library
Marine Corps Air Station
Cherry Point, NC 28533-5030 1 copy

Commanding Officer
Naval Aviation Depot
Attn: Technical Library
North Island
San Diego, CA 92135 1 copy

Commander
Naval Aviation Depot Operations Center
Patuxent River, MD 20670 1 copy

Commander
David Taylor Research Center
Attn: Technical Library
Bethesda, MD 20034 1 copy

Commanding Officer
Naval Air Systems Command
Attn: AIR-530
Washington, D.C. 20361 3 copies

Commanding Officer
Naval Air Systems Command
Attn: AIR-5302
Washington, D.C. 20361 1 copy

Commanding Officer
Naval Air Systems Command
Attn: AIR-53021
Washington, D.C. 20361 1 copy

Commanding Officer
Naval Air Systems Command
Attn: AIR-53022
Washington, D.C. 20361 1 copy

Commanding Officer
Naval Air Systems Command
Attn: AIR-53023
Washington, D.C. 20361 1 copy

Federal Aviation Administration
Technical Center
Attn: Mr. L. Neri, Code ACT-330
Atlantic City, NJ 08405 1 copy

Federal Aviation Administration
Technical Center
Attn: Mr. M. Ciafa, Code ACT-330
Atlantic City, NJ 08405 1 copy

Commanding Officer
Naval Aviation Depot
Attn: Technical Library
Jacksonville, FL 32212 1 copy

Commanding Officer
Naval Aviation Depot
Attn: Technical Library
Pensacola, FL 32508 1 copy

Commander
Naval Post Graduate School
Attn: Prof. K. Challenger
Monterey, CA 95940 1 copy

Officer in Charge
David Taylor Research Center
Attn: 2814/T. Montemarano
Annapolis, MD 21402 1 copy

Naval Surface Weapons Center
White Oak Laboratory
Attn: Technical Library
Silver Spring, MD 20910 1 copy

Commanding Officer
Naval Air Systems Command
Attn: AIR-00D4
Washington, D.C. 20361 1 copy

Commanding Officer
Naval Air Systems Command
Attn: AIR-931B
Washington, D.C. 20361 1 copy

NAVAIRDEVCEN
Attn: Code 8131
Warminster, PA 18974-5000 2 copies